

Figure 3. The Recruitment of FAAP20 to ICLs Requires Its Ubiquitin-Binding Activity, RNF8 and UBC13, but Not RNF168

(A) Images showing that GFP-tagged FAAP20 protein in HeLa cells was recruited to psoralen-induced ICLs at various time points after laser activation. The arrows indicate positive recruitment signals.

Molecular Cell

A Ubiquitin Cascade in Fanconi Anemia Network

enzyme specific for K63 linkage and a partner of RNF8, from HeLa cells by two different siRNAs. The recruitment of GFP-FAAP20 to ICLs was eliminated, as it was in RNF8-depleted cells (Figures 3E and 3F, and Figure S3C), indicating that K63-linked polyubiquitin produced by RNF8-UBC13 is the primary signal for FAAP20 recruitment.

K63-linked ubiquitin chains formed at DSBs are stable and can last at least 4 hr, in contrast to K48-linked chains that are unstable and diminish within 1 hr (Feng and Chen, 2012). The GFP-FAAP20 remained at ICLs for at least 2.5 hr (Figure 3A), consistent with the notion that it recognizes the stable K63-linked chains.

RNF168 Is Largely Dispensable for FAAP20 Recruitment

RNF168 is the second E3 ubiquitin ligase that accumulates at damaged chromatin and amplifies K63-linked polyubiquitination initiated by RNF8-UBC13. Interestingly, the recruitment of GFP-FAAP20 to ICLs was observed in majority of cells depleted of RNF168 by two different siRNAs (83% and 78% for siRNF168-treated cells, compared to 95% for control cells) (Figures 3E and 3F, and Figure S3D). As a control, the recruitment of RNF168 itself to ICLs was eliminated by the same siRNAs (see Figures 5D and 5E). Therefore, RNF168-mediated amplification of the K63 ubiquitin signal is largely dispensable for recruitment of FAAP20.

The Ubiquitin-Binding Activity of FAAP20 Is Required for Normal Recruitment of the FA Core Complex and FANCD2 to ICLs

We studied whether the RNF8-FAAP20 cascade controls recruitment of the FA core complex and FANCD2 to ICLs. We observed recruitment of both FANCA and FANCD2 to ICLs (Figure 4A). The data are in agreement with earlier findings that FA proteins function at ICLs (Ben-Yehoyada et al., 2009; Knipscheer et al., 2009; Shen et al., 2009; Yan et al., 2010). Importantly, the recruitment of both FANCA and FANCD2 was strongly diminished in cells depleted of FAAP20 (Figures 4A and 4B), indicating that FAAP20 is required for normal recruitment of the FA core and ID complexes to ICLs. Notably, introduction of an siRNA-resistant version of FAAP20 into FAAP20 siRNA-treated cells partially rescued the recruitment of FA core complex and FANCD2, whereas the FAAP20-D164A mutant failed to rescue (Figures 4C–4E; and Figure S4A). In fact, even when cells were treated with control siRNA, those expressing FAAP20-D164A mutant had 90% reduction of FANCA and 40% reduction of FANCD2 recruitment compared those expressing wild-type FAAP20, indicating that the UBZ mutant acts dominant-negatively to inhibit the recruitment process. The data suggest that the ubiquitin-binding activity of FAAP20 is needed for recruitment not only

of itself (Figures 3B–3D) but also of the FA core complex and FANCD2.

The Ubiquitin-Binding Activity of FAAP20 Is Required for Normal Activation of the FA Pathway

We investigated whether the ubiquitin-binding activity of FAAP20 is needed for FA pathway activation using FAAP20^{-/-} DT40 cells. The FAAP20^{-/-} cells had a lower level of monoubiquitinated FANCD2 (Figure 4F and Figure S4B) as well as a reduced number of FANCD2 nuclear foci in response to MMC treatment (Figures 4G and 4H); introduction of wild-type FAAP20 largely corrected both defects. In contrast, introduction of FAAP20 carrying either C147A or D164A substitutions failed to correct these defects (Figures 4F–4H, and Figures S4C and S4D). Because both mutants lack ubiquitin-binding activity, the data suggest that this activity of FAAP20 is required for optimal activation of the FA pathway.

A FAAP20 mutant that lacked the UBZ domain coimmunoprecipitated normally with FANCA (Figures S4E and S4F), suggesting that the failure of the UBZ domain mutants to restore the FA pathway is not due to their inability to assemble into the FA core complex. Another FAAP20 mutant lacking the N-terminal 65 residues failed to coimmunoprecipitate with FANCA (Figures S4E and S4F), indicating that this region is required for FAAP20 assembly into the core complex.

RNF8 and Its Ubiquitinated Product Accumulate at ICLs Earlier Than FA Proteins

RNF8 accumulates rapidly at DSBs to promote K63-linked ubiquitination on H2A-type histones (Huen et al., 2007; Kolas et al., 2007; Martijn et al., 2009; Wang and Elledge, 2007). We found that RNF8 and its product, ubiquitinated H2A, accumulated at laser-activated ICLs within minutes after photoactivation (Figures 5A and 5B). The appearance of RNF8 preceded that of ubiquitinated H2A (approximately 1 min versus 3 min) (Figure 5A), consistent with a sequential process in which RNF8 is first recruited by an upstream signal and then ubiquitinates H2A at the site of damage.

The accumulation of RNF8 and ubiquitinated H2A at ICLs precedes that of FANCA and FANCD2 (1 and 3 min versus 5 and 10 min) (Figure 5A), suggesting that RNF8-initiated ubiquitination signals (ubiquitinated H2A or other substrates) act earlier in a cascade to recruit FANCA proteins to ICLs.

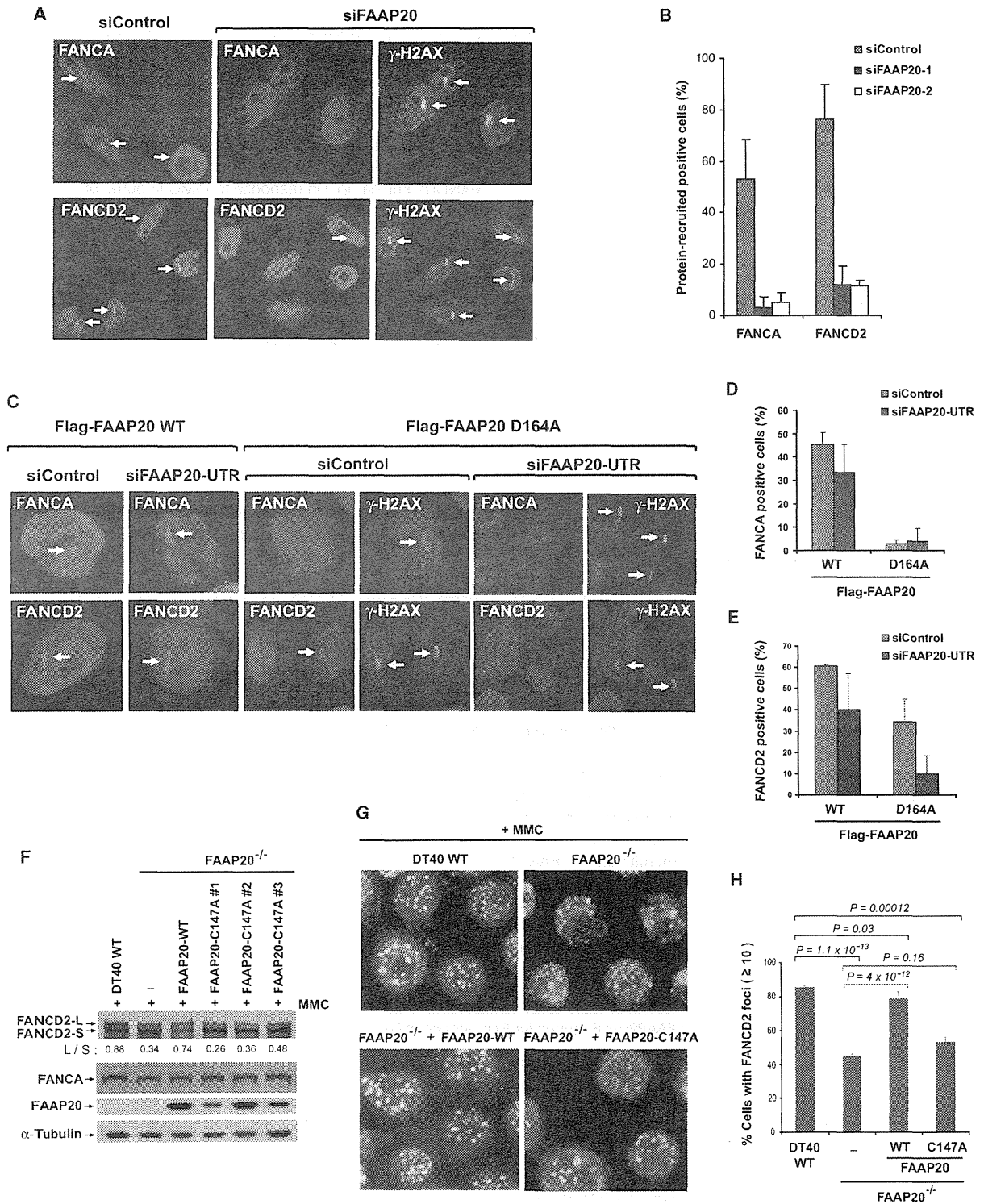
The Recruitment of FANCA and FANCD2 to ICLs Requires RNF8

The data above suggested a hierarchy in control of FA proteins: RNF8 is required for recruitment of FAAP20, which is in turn needed for recruitment of FA core complex and FANCD2.

(B and C) Images (B) and a graph (C) show that GFP-FAAP20 wild-type (WT) was recruited to ICL sites, but the GFP-FAAP20-D164A mutant was not. Immunostaining of γ -H2AX marks the areas targeted by the laser and also serves as a control to show a positive DNA damage response. Error bars in (C) are standard deviations.

(D) (Top panel) Schematic representation of the plasmid substrates used in the eChIP assay. The presence of psoralen-ICL is indicated. (Bottom panel) A graph from eChIP shows that FAAP20 wild-type (WT) protein was enriched about 4-fold at the ICL, whereas FAAP20-D164A mutant was not. Error bars represent standard deviations from three independent experiments.

(E and F) Images (E) and graphs (F) show the recruitment of GFP-FAAP20 to ICLs in HeLa cells transfected with two different siRNAs against RNF168, RNF8, or UBC13, respectively. Error bars in (F) are standard deviations (see also Figure S3).



Molecular Cell

A Ubiquitin Cascade in Fanconi Anemia Network

The data predict that RNF8 should also be required for recruitment of FA core complex and FANCD2. In agreement with this notion, depletion of RNF8 by two different siRNAs in HeLa cells not only disrupted induction of ubiquitinated H2A but also substantially reduced the accumulation of FANCA and FANCD2 at ICLs (Figures 5B and 5C). These data suggest that RNF8 acts upstream of FA core complex and FANCD2 to promote their recruitment to ICLs.

RNF168 Affects Efficiency of the Recruitment of FANCD2 Proteins to ICLs

Like RNF8, RNF168 also accumulated at ICLs, and its appearance was after RNF8 but before FANCA and FANCD2 (Figures 5A and 5D). However, depletion of RNF168 by two different siRNAs had only a modest effect on recruitment of FANCA and FANCD2: about 50% reduction for the former and 20% for the latter (Figure 5E). This is in contrast to the depletion of RNF8, which reduced recruitment of FANCA and FANCD2 by about 90% and 80%, respectively. These data are reminiscent of the findings that RNF168 depletion does not significantly affect recruitment of GFP-FAAP20 (Figures 3E and 3F). Thus, while RNF8 plays a critical role for recruitment of FANCD2 proteins to ICLs, RNF168 only affects the efficiency of the recruitment.

RNF8 Is Dispensable for Recruitment of FANCM to ICLs

We have previously shown that most FANCM and its DNA binding partner MHF (about 90%) do not associate with the FA core complex but are present in the distinct FANCM-MHF complex that lacks FANCA and other FANCD2 proteins. Moreover, the recruitment of FANCM-MHF to laser-activated psoralen ICLs only occurs in S phase cells (Yan et al., 2010). This is in contrast to recruitment of RNF8, GFP-FAAP20, FANCA, and FANCD2 that occurred in most (80% or more) unsynchronized HeLa cells (Figure 3C and Figure 5A; less than 20% of these cells are in S phase [data not shown]). The data imply that recruitment of FANCM-MHF in the S phase is different from the RNF8-dependent recruitment of FANCA and FANCD2, which can occur independently of cell-cycle phase. In support of this notion, the recruitment of FANCM was unaffected in RNF8-depleted cells (Figures 5B and 5C), in contrast to recruitment of FANCA and FANCD2, which was disrupted. Together, the data suggest that RNF8-mediated ubiquitination is dispensable for FANCM recruitment during S phase.

RNF8 Promotes Efficient Activation of the FA Network and Works in the Same Pathway as the FA Core Complex in Cellular Resistance to ICLs

Our findings that RNF8 is required for recruitment of FANCD2 proteins to ICLs prompted us to study if it is also needed for activation of the FA network. We found that HeLa cells depleted of RNF8 by two different siRNAs exhibited a reduced level of monoubiquitinated FANCD2 (Figure 6A) and a decreased number of FANCD2 nuclear foci in response to MMC (Figures 6B and 6C). The reduced FANCD2 monoubiquitination was not due to inability of the depleted cells to enter S phase, because the percentage of S phase cells in RNF8-depleted cells was comparable to that of control cells (Figure S5A). Moreover, RNF8-depleted cells displayed increased sensitivity to MMC (Figures S5B and S5C). These features resemble those of cells deficient in FA core complex and suggest that RNF8 is required for normal function of the FA pathway.

Importantly, cells doubly depleted of both RNF8 and FANCA exhibited MMC sensitivity similar to that of single gene-depleted cells (Figures 6D and 6E), suggesting that RNF8 and FA core complex act in the same pathway to resist MMC-induced DNA damage.

The RNF8-FAAP20 Cascade Is Required for Recruitment of FA Core Complex and FANCD2 to DSBs

The FA network can be activated not only by ICLs but also by other DNA damage, including DSBs (Garcia-Higuera et al., 2001). We asked if FANCD2 proteins are recruited to DSBs, and if they do, whether their recruitment also depends on the RNF8-FAAP20 cascade. We found that both FANCA and FANCD2 were recruited to laser-activated DSBs (Figures S6A and S6B). Importantly, recruitment of both FANCD2 proteins was strongly abrogated in cells depleted of either FAAP20 (Figures S6A and S6B) or RNF8 (Figures S6C and S6D). The data suggest that the RNF8-FAAP20 cascade may be part of a general pathway that governs recruitment of FANCD2 proteins to multiple forms of DNA damage.

DISCUSSION

RNF8 and FAAP20 Constitute a Ubiquitin Signaling Cascade

Phosphorylation of several subunits of the FA core complex by ATR and its downstream kinase CHK1 has been shown to regulate monoubiquitination of FANCD2, a key function of the

Figure 4. The Ubiquitin-Binding Activity of FAAP20 Is Required for Recruitment of FA Core Complex and FANCD2 and for Normal Activation of the FA Pathway

(A and B) Images (A) and a graph (B) show that HeLa cells depleted of FAAP20 by two siRNAs are deficient in the recruitment of FANCA and FANCD2 to ICL sites. Immunostaining of γ -H2AX indicates the areas targeted by the laser and also serves as a control to show a positive DNA damage response. The positive recruitment signals are indicated by arrows. Error bars in (B) are standard deviations.

(C–E) Images (C) and graphs (D and E) show the recruitment of FANCA and FANCD2 at ICLs in HeLa cells stably expressing an siRNA-resistant version of Flag-FAAP20 wild-type (WT) or D164A mutant. These cells were treated with either a nontargeting siRNA (siControl) or a siRNA targeting the 3' untranslated region of human FAAP20 (siFAAP20-UTR). Error bars in (D) and (E) are standard deviations.

(F) Immunoblotting shows the levels of monoubiquitinated (L) and nonubiquitinated (S) FANCD2 in lysates from various DT40 cells (wild-type [WT], FAAP20^{-/-} cells, and FAAP20^{-/-} cells complemented with human FAAP20 wild-type [WT] and C147A mutant version [three independent clones]). Cells were treated with 500 ng/ml MMC for 6 hr.

(G and H) Immunostaining images (G) and a graph (H) show FANCD2 nuclear foci in various DT40 cells treated with MMC. The error bars in (H) are standard deviations. p values between different cell lines are shown (see also Figure S4).

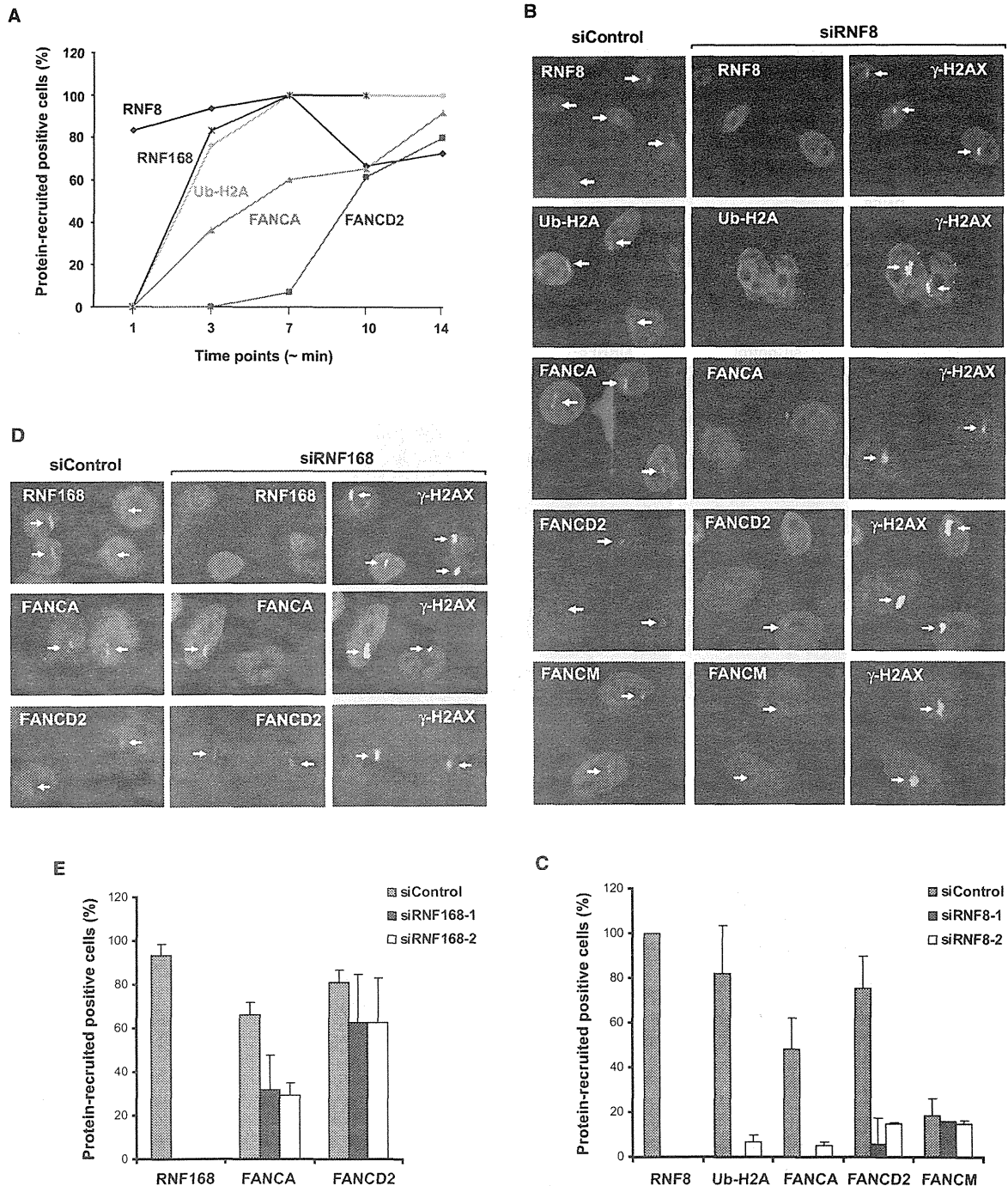


Figure 5. RNF8 Is Required for Recruitment of FANCA and FANCD2 to ICLs, but Not for FANCM Recruitment

(A) A time course study shows the sequential recruitment of RNF8, RNF168, Ub-H2A, FANCA, and FANCD2 to psoralen-induced ICLs after laser activation. (B and C) Images (B) and a graph (C) show that HeLa cells depleted of RNF8 by two siRNAs are deficient in accumulation of ubiquitinated H2A (Ub-H2A), FANCA, and FANCD2 at ICLs; but they are normal in accumulation of FANCM. Immunostaining of γ -H2AX marks the areas targeted by the laser and also serves as a control to show a positive DNA damage response. The recruitment signals are indicated by arrows. Error bars are standard deviations. (D and E) The same as described in (B) and (C), except siRNAs targeting RNF168 are used.

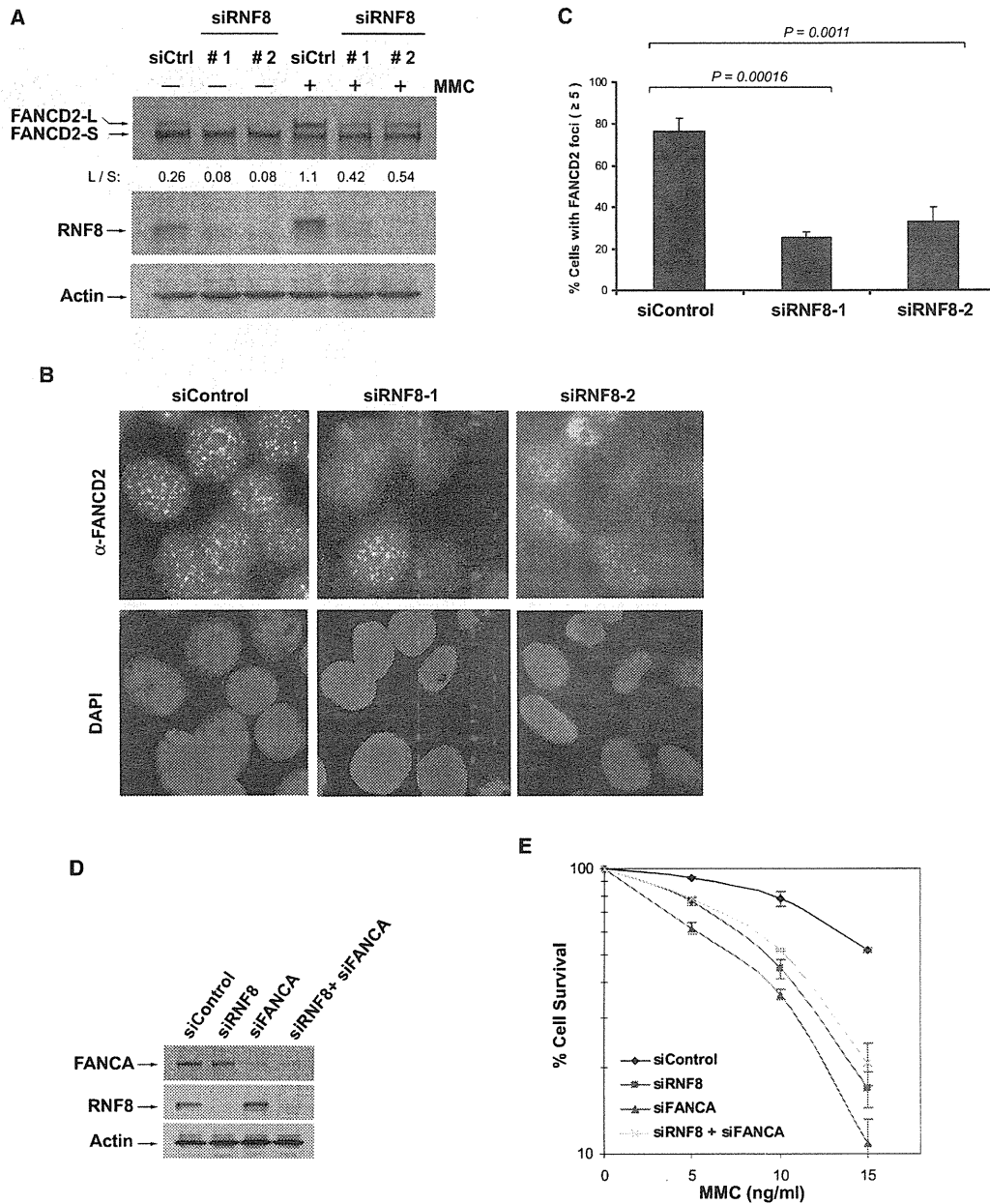


Figure 6. RNF8 Is Required for Efficient FANCD2 Monoubiquitination and Focus Formation and Works in the Same Pathway as the FA Core Complex in Cellular Resistance to ICLs

(A) Immunoblotting shows that HeLa cells depleted of RNF8 by two different siRNAs have a reduced level of monoubiquitinated FANCD2 in the absence or presence of MMC (60 ng/ml for 16 hr).

(B and C) Immunostaining (B) and a graph (C) show that HeLa cells depleted of RNF8 by two siRNAs have a decreased number of FANCD2 nuclear foci in the presence of MMC. Error bars are standard deviations. p values are shown in the top.

(D) Immunoblotting shows the levels of FANCA and RNF8 in lysates from HeLa cells treated with various siRNAs as indicated.

(E) Clonogenic survival assays of HeLa cells depleted of RNF8 or FANCA or doubly depleted of both by siRNAs following the treatment with MMC. The mean surviving percentages with standard error of the mean (SEM) from three independent experiments are shown (see also Figure S5).

Models for the recruitment of FA core and ID complexes to ICLs

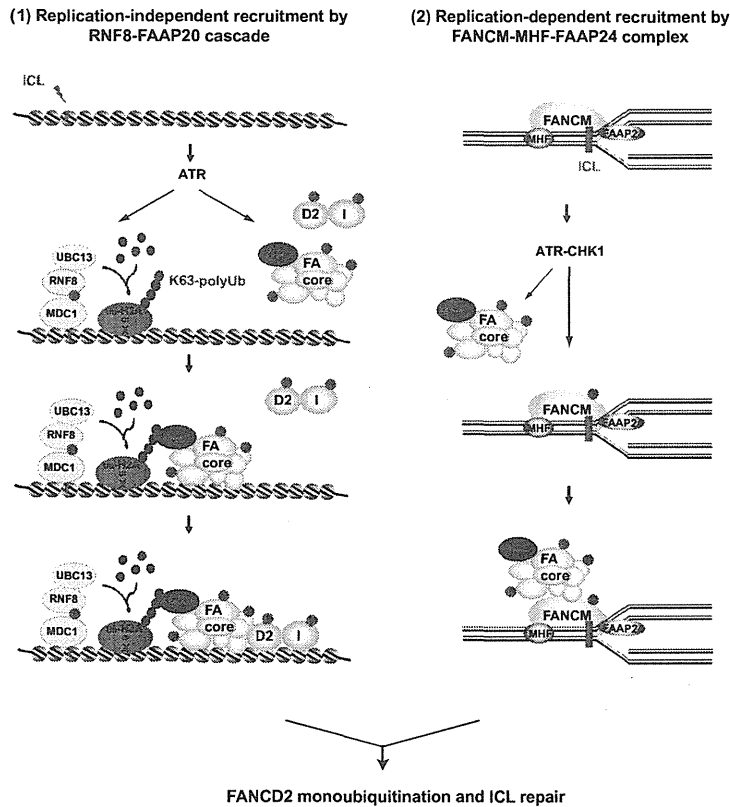


Figure 7. Models for the Recruitment of FA Core Complex and FANCD2 to ICLs by Two Different Pathways

The first pathway is replication independent and controlled by the RNF8-FAAP20 cascade. In keeping with the literature on the activation of the DNA damage response by DSBs, ICLs may activate ATR, which can phosphorylate MDC1 and FANCD2 proteins. RNF8 and UBC13 are recruited to initiate K63-linked polyubiquitination of histone H2A and other substrates (marked by "X") in surrounding chromatin, which are recognized by the UBZ domain of FAAP20 to trigger the recruitment of FA core complex. The FA ID complex is possibly recruited by interacting with the FA core complex. The second pathway is replication dependent and governed by FANCM-MHF-FAAP24 complex. In S phase, FANCM-MHF-FAAP24 complex recognizes ICL-stalled replication forks, activates ATR and CHK1 (Collis et al., 2008), and recruits the FA core complex by direct protein-protein interactions. Both pathways lead to FANCD2 monoubiquitination, the key step of the FA network (see also Figure S6).

substrates in chromatin flanking the lesions. The ubiquitinated H2A (and perhaps other ubiquitinated molecules) then interacts with the UBZ domain of FAAP20 to recruit the FA core complex to damaged chromatin. Finally, FANCD2 is recruited, possibly by interacting with the FA core complex already bound at the ICLs. This model is supported by the siRNA data showing that RNF8 depletion

core complex (Collins et al., 2009; Wang et al., 2007) (Figure 7). Here we show that the core complex is also governed by a ubiquitin signaling cascade, which is initiated by RNF8 and its partner UBC13, and mediated by FAAP20, a component of the FA core complex. RNF8 and UBC13 act upstream of this cascade, because depletion of either protein abolished the recruitment of GFP-FAAP20 to ICLs. Conversely, FAAP20 functions downstream, as FAAP20 can bind K63-linked polyubiquitin, the product of RNF8-UBC13, in vitro; and the FAAP20 mutant defective in this ubiquitin-binding activity failed to accumulate at ICLs in vivo. Consistent with the proposed role of RNF8 in regulating FA network, our epistasis analyses showed that RNF8 and FANCA work in the same pathway to resist MMC-induced cell killing.

The RNF8-FAAP20 Cascade is Essential for Recruitment of FA Core Complex to ICLs and for Efficient Activation of the FA Pathway

Our time course analyses revealed a sequential accumulation process of repair proteins at ICLs (Figure 5A). This sequential process suggests a model of how RNF8 regulates the recruitment of FANCD2 proteins (Figure 7). In response to ICLs, RNF8 is recruited to the damage site, where it works with UBC13 to catalyze K63-linked ubiquitination of histone H2A and possibly other

disrupted accumulation of all downstream proteins at ICLs, and that FAAP20 depletion reduced FANCA and FANCD2 recruitment. It is also supported by the evidence that the ubiquitin-binding activity of FAAP20 is needed for recruitment of FANCA and FANCD2.

The RNF8-FAAP20 cascade also plays a regulatory albeit nonessential role in modulating the efficiency of FANCD2 monoubiquitination, a key step of the FA network. This is evidenced by observations that HeLa cells depleted of either RNF8 or FAAP20, and DT40 cells inactivated of FAAP20, all displayed reduced levels of MMC-induced FANCD2 monoubiquitination and redistribution to nuclear foci.

FANCM is Recruited to ICLs through a Pathway Independent of RNF8

Why is the RNF8-FAAP20 cascade essential for recruitment of FA core complex to psoralen-activated ICLs but nonessential for MMC-induced FANCD2 monoubiquitination? One explanation is that there exists another pathway independent of the RNF8-FAAP20 cascade that can also promote FANCD2 monoubiquitination (Figure 7). It should be pointed out that ICLs generated by psoralen and MMC are structurally different so that they may be detected by distinct mechanisms, leading to different responses (Muniandy et al., 2010). The psoralen ICLs distort DNA duplex

Molecular Cell

A Ubiquitin Cascade in Fanconi Anemia Network

so that they can be rapidly detected by DNA damage sensors in any phase of the cell cycle to activate the RNF8-FAAP20 cascade. In contrast, MMC ICLs do not significantly distort DNA duplex, so they may remain largely undetected until S phase, when they block progression of replication forks. The blocked forks may be recognized by FANCM-MHF (and possibly FAAP24), which recruits the FA core complex through direct protein-protein interactions. In agreement with this notion, the recruitment of FANCM-MHF to ICLs of psoralen occurred only during S phase (Yan et al., 2010) and was unaffected when RNF8 was depleted (Figures 5B and 5C). Thus, at least two pathways regulate the FA core complex recruitment: one is replication independent, and the other one is replication dependent. Only the first one depends on the RNF8-FAAP20 cascade, whereas the latter one depends on FANCM and its DNA-binding partners. Cells deficient in either pathway are partially defective in FANCD2 monoubiquitination. We predict that only when both pathways are disrupted will FANCD2 monoubiquitination be eliminated.

K63-Linked Polyubiquitin Generated by RNF8-UBC13 Signals FAAP20 Recruitment

RNF8 can promote ubiquitination of both K63- and K48-linked chains at DSBs (Feng and Chen, 2012; Lok et al., 2011). We found that the UBZ domain of FAAP20 can bind both chains but has a preference for K63 linkage. Our findings that cells depleted of UBC13, the E2 enzyme specific for K63-linked polyubiquitination, are completely deficient in recruiting GFP-FAAP20 to ICLs indicate that the K63 linkage is the primary signal. In support of this notion, inhibition of K63-linked polyubiquitination sensitizes cells to agents that induce ICLs (Chiu et al., 2006); and cells deficient in UBC13 are sensitive to ICL-inducing drugs (Zhao et al., 2007). The observation that K48 chains are bound by FAAP20 *in vitro*, but do not appear to be effective binding partners *in vivo* (because UBC13 depletion eliminated FAAP20 recruitment even though K48 chains would be present), suggests that recognition of K48 by FAAP20 may be suppressed *in vivo*, perhaps outcompeted by proteins with higher affinity for K48.

RNF168 Affects Efficiency of the Recruitment of FA Proteins to ICLs

RNF8 and RNF168 ubiquitin ligases work coordinately to catalyze K63-linked polyubiquitination at chromatin regions surrounding DSBs or UV-induced damage sites, and both are required for recruitment of several downstream repair molecules. Our data suggest that the RNF8-initiated K63-linked polyubiquitination signal is sufficient for recognition by the UBZ domain of FAAP20, leading to recruitment of FA core complex and FANCD2; further amplification of the signal by RNF168 is not necessary but can increase the amount of the recruited FANCD2 proteins. Notably, this selective dependence on RNF8 over RNF168 has been observed for accumulation of RAD51 recombinase at ssDNA lesions in response to replication stress induced by hydroxyurea (Sy et al., 2011). Perhaps cells may have developed different ubiquitin-binding domains (UBDs) to distinguish different K63-linked polyubiquitin signals produced by RNF8 and RNF168. The FAAP20-UBZ domain may

represent one type of UBDs that can bind shorter K63-linked chains generated by RNF8, whereas the UBDs in some other proteins may only recognize elongated K63 chains produced by RNF168.

The Ubiquitin-Binding Activity of FAAP20 is Essential for Recruitment of FA Core Complex to ICLs and for Optimal Activation of the FA Pathway

While our manuscript was under revision, three groups independently reported that FAAP20 is part of the FA core complex and required for optimal activation of the FA pathway (Ali et al., 2012; Kim et al., 2012; Leung et al., 2012), consistent with our findings. However, the conclusions regarding the ubiquitin-binding activity of FAAP20 are controversial. First, Ali et al. showed that FAAP20 does not bind monoubiquitin, in agreement with our data, whereas Kim et al. proposed that FAAP20 binds Rev1, and this binding is enhanced by monoubiquitination of Rev1. However, examination of the data from Kim et al. suggests that FAAP20 appears to bind better to nonubiquitinated than monoubiquitinated Rev1 (the ratio between the nonubiquitinated and monoubiquitinated form was increased in their FAAP20 immunoprecipitate compared to the pre-IP extract, their Figure 4C, lane 7 versus lane 3); and FAAP20 with mutated UBZ domain can still bind Rev1 (their Figure 4C, lane 8). One interpretation, which fits data from all groups, is that FAAP20 may bind nonubiquitinated Rev1 through a ubiquitin-independent mechanism, and this binding may be decreased by monoubiquitination. Second, Ali et al., using FAAP20-depleted HeLa cells, concluded that the ubiquitin-binding activity of FAAP20 is necessary for normal activation of the FA pathway, whereas Leung et al., using FAAP20-inactivated HCT116 cells, concluded that it is dispensable. Our data from FAAP20-knockout DT40 cells and FAAP20-depleted HeLa cells suggest that this activity is not only important for normal activation of the FA pathway but also critical for recruitment of the FA core complex to ICLs. The lack of importance for this activity in HCT116 cells might be because this cell line carries mutations in MRE11 and MLH1, which are involved in activation of ATR (Nam and Cortez, 2011), resulting in aberrant response to replication stress (Wen et al., 2008). We found that recruitment of FA proteins to ICLs in HCT116 cells is about 50% lower compared to that in HeLa cells (data not shown), suggesting that the RNF8-FAAP20 cascade may be inefficiently utilized and thus less important in this cell line.

In summary, our data suggest that the FA core complex is governed not only by phosphorylation but also by the RNF8-FAAP20 ubiquitin cascade. Our data showing that the recruitment of the FA core complex and FANCD2 to DSBs also depends on RNF8 and FAAP20 suggest that this cascade can respond to many forms of DNA damage.

EXPERIMENTAL PROCEDURES

Cell Lines

Human HeLa and HEK293 cells were grown in DMEM medium supplemented with 10% fetal bovine serum (FBS). Chicken DT40 cells were grown in RPMI-1640 medium supplemented with 10% fetal calf serum, 1% chicken serum, 10 mM HEPES, and 1% penicillin-streptomycin mixture in a 5% CO₂ incubator at 39.5°C. HeLa cells stably expressing Flag-FAAP20 WT and D164A mutant used in eChIP assay were kindly provided by Dr. A.R. Meetei (Ali et al., 2012).

Antibodies

An anti-human FAAP20 antibody was raised against a chimeric protein containing a region of human FAAP20 (aa 67–180) fused to maltose-binding protein (New England Biolabs). An anti-chicken FANCA antibody was raised against a chimeric protein containing a region of chicken FANCA (aa 1698–1944) fused to maltose-binding protein. Anti-chicken FANCD2 and FANCI antibodies were generated in rabbits by injection of recombinant whole-chicken FANCD2 protein (Yamamoto et al., 2011) and partial chicken FANCI protein (aa 1–125), respectively. An anti-RNF168 antibody was kindly provided by Dr. D. Durocher. Anti-RNF8 and anti-UBC13 antibodies were purchased from Abcam. An anti-ubiquitinated histone H2A antibody was purchased from Millipore. An anti-ubiquitin antibody was purchased from Cell Signaling. Other antibodies have been previously described (Yan et al., 2010).

Protein Recruitment to Laser-Induced Localized ICLs

We followed a previous protocol to detect proteins recruited at laser-induced localized ICLs (Muniandy et al., 2009). Briefly, cells were seeded in a 35 mm glass bottom culture dish (MatTek) and were incubated with 6 μ M trioxalen at 37°C for 20 min prior to laser treatment. Localized irradiation was performed using the Nikon Eclipse TE2000 confocal microscope equipped with an SRS NL100 nitrogen laser-pumped dye laser (Photonics Instruments, St Charles, IL) that fires 5 ns pulses with a repetition rate of 10 Hz at 365 nm, with a power of 0.7 nW, measured at the back aperture of the 60 \times objective. The laser was directed to a specified rectangular region of interest (ROI) within the nucleus of a cell visualized with a Plan Fluor 60 \times /NA 1.25 oil objective. The laser beam was oriented by galvanometer-driven beam displacers and fired randomly throughout the ROI until the entire region was exposed. Throughout an experiment, cells were maintained at 37°C, 5% CO₂, and 80% humidity using an environmental chamber. Cells were fixed immediately in freshly prepared 4% formaldehyde in PBS for 10 min at room temperature, followed by immunostaining.

Detecting Proteins Recruited to a Site-Specific Psoralen-ICL by eChIP

The eChIP was carried out as described (Shen et al., 2009). Percentages of relative enrichment of FAAP20 at the ICL site were arrived by normalizing comparative concentration (from real-time PCR) of each sample with that of its input.

siRNA Experiments

HeLa cells were transfected with siRNA oligos using Lipofectamine RNAi MAX (Invitrogen) according to the manufacturer's protocol. The siRNA oligos used are listed in the Supplemental Information.

Expression and Purification of GST-Fusion Proteins from *E. coli*

The expression plasmid for GST-FAAP20-UBZ domain (pGEX-FAAP20-UBZ) was constructed by cloning a region of human FAAP20 that includes the UBZ domain into the BamHI and EcoRI sites of pGEX-2TK. *E. coli* Rosetta (Novagen) cells carrying pGEX-UBZ-wild-type construct or its mutant versions were grown at 30°C to OD₆₀₀ of 0.4–0.5, and 200 μ M ZnCl₂ (final concentration) was added to culture. When OD₆₀₀ reached 0.6–0.8, cells were induced with 0.2 mM IPTG at 30°C for 3 hr. Cell pellets were resuspended in lysis buffer (25 mM sodium phosphate [pH 8.0], 300 mM NaCl, 10% glycerol) containing lysozyme, DNase I, benzonase, and complete EDTA-free protease inhibitor cocktail (Roche). The mixture was sonicated, and the lysed cells were cleared by centrifugation at 16,000 rpm for 35 min. The supernatant was then incubated for 1 hr with glutathione Sepharose beads (GE Healthcare). After washing with 10 column volumes (CV) of lysis buffer followed by 10 CV of wash buffer (25 mM sodium phosphate [pH 8.0], 300 mM NaCl), the bound GST-fusion proteins were eluted in 10 CV of elution buffer (25 mM sodium phosphate [pH 8.0], 150 mM NaCl, 30 mM glutathione). Peak fractions were pooled and dialyzed with dialysis buffer (25 mM sodium phosphate [pH 7.0], 150 mM NaCl).

In Vitro Ubiquitin-Binding Assay

Equal amounts (10 μ g) of purified GST-UBZ fusion proteins or GST protein alone were incubated with 10 μ l of ubiquitin agarose (Boston Biochem) in

binding buffer (25 mM HEPES [pH 7.9], 150 mM NaCl, 20 μ M ZnCl₂, 0.1% Tween 20, 5 mM β -mercaptoethanol) at 4°C for 1 hr. After washing with binding buffer four times, beads were boiled in SDS gel loading buffer, and the samples were analyzed by Coomassie blue staining.

GST Pull-Down Assay

Glutathione Sepharose beads (GE Health) with 10 μ g of purified GST-UBZ fusion proteins or GST protein alone were incubated with different amounts of K63- or K48-linked polyubiquitin substrates (Boston Biochem) in binding buffer (described above) at 4°C overnight. Because the K63-linked polyubiquitin substrate contains a higher proportion of long chains than the K48-linked substrate, we used 10 μ g of K48-linked polyubiquitin and 0.4 μ g of K63-linked polyubiquitin in reactions of Figure 2C. This allows the level of K48-linked long chains to be comparable to that of the K63-linked long chains. In Figures 2E and 2F, 7 μ g of K63-linked ubiquitin and 10 μ g of K48-linked ubiquitin were used, respectively. After washing with the binding buffer four times, beads were boiled in SDS gel loading buffer and the samples were analyzed by immunoblotting.

Gel Filtration, Immunoprecipitation, and Protein Identification

We followed the protocol as described (Yan et al., 2010). Briefly, we fractionated HeLa nuclear extract by Superose 6 gel filtration chromatography, pooled the peak fractions containing FANCA, and immunoprecipitated the core complex with a FANCA antibody. The eluted immunoprecipitates were subjected to silver staining, mass spectrometry, and immunoblotting analyses.

Detailed experimental materials and methods can be found in the Supplemental Information.

ACCESSION NUMBERS

The NCBI accession number for the FAAP20 sequence reported in this paper is NP_872339.2 (C1orf86 isoform 2).

SUPPLEMENTAL INFORMATION

Supplemental Information includes six figures, Supplemental Experimental Procedures, and Supplemental References and can be found with this article online at doi:10.1016/j.molcel.2012.05.026.

ACKNOWLEDGMENTS

We thank Drs. D. Durocher, M. Huen, and A.R. Meetei for reagents, and Dr. David Schlessinger for critical reading of the manuscript. This work was supported in part by the Intramural Research Program of the National Institute on Aging (AG000688-07), National Institutes of Health.

Received: November 18, 2011

Revised: May 1, 2012

Accepted: May 17, 2012

Published online: June 14, 2012

REFERENCES

- Al-Hakim, A., Escibano-Diaz, C., Landry, M.C., O'Donnell, L., Panier, S., Szilard, R.K., and Durocher, D. (2010). The ubiquitous role of ubiquitin in the DNA damage response. *DNA Repair (Amst.)* 9, 1229–1240.
- Ali, A.M., Pradhan, A., Singh, T.R., Du, C., Li, J., Wahengbam, K., Grassman, E., Auerbach, A.D., Pang, Q., and Meetei, A.R. (2012). FAAP20: a novel ubiquitin-binding FA nuclear core complex protein required for functional integrity of the FA-BRCA DNA repair pathway. *Blood* 119, 3285–3294.
- Ben-Yehoyada, M., Wang, L.C., Kozekov, I.D., Rizzo, C.J., Gottesman, M.E., and Gautier, J. (2009). Checkpoint signaling from a single DNA interstrand crosslink. *Mol. Cell* 35, 704–715.
- Bomar, M.G., Pai, M.T., Tzeng, S.R., Li, S.S., and Zhou, P. (2007). Structure of the ubiquitin-binding zinc finger domain of human DNA Y-polymerase eta. *EMBO Rep.* 8, 247–251.

Molecular Cell

A Ubiquitin Cascade in Fanconi Anemia Network

- Chiu, R.K., Brun, J., Ramaekers, C., Theys, J., Weng, L., Lambin, P., Gray, D.A., and Wouters, B.G. (2006). Lysine 63-polyubiquitination guards against translesion synthesis-induced mutations. *PLoS Genet.* 2, e116. 10.1371/journal.pgen.0020116.
- Collins, N.B., Wilson, J.B., Bush, T., Thomashevski, A., Roberts, K.J., Jones, N.J., and Kupfer, G.M. (2009). ATR-dependent phosphorylation of FANCA on serine 1449 after DNA damage is important for FA pathway function. *Blood* 113, 2181–2190.
- Collis, S.J., Ciccio, A., Deans, A.J., Horejsi, Z., Martin, J.S., Maslen, S.L., Skehel, J.M., Elledge, S.J., West, S.C., and Boulton, S.J. (2008). FANCM and FAAP24 function in ATR-mediated checkpoint signaling independently of the fanconi anemia core complex. *Mol. Cell* 32, 313–324.
- Cordier, F., Grubisha, O., Traincard, F., Veron, M., Delepiepierre, M., and Agou, F. (2009). The zinc finger of NEMO is a functional ubiquitin-binding domain. *J. Biol. Chem.* 284, 2902–2907.
- Feng, L., and Chen, J. (2012). The E3 ligase RNF8 regulates KU80 removal and NHEJ repair. *Nat. Struct. Mol. Biol.* 19, 201–206.
- Garcia-Higuera, I., Taniguchi, T., Ganesan, S., Meyn, M.S., Timmers, C., Hejna, J., Grompe, M., and D'Andrea, A.D. (2001). Interaction of the Fanconi anemia proteins and BRCA1 in a common pathway. *Mol. Cell* 7, 249–262.
- Huang, M., Kim, J.M., Shiotani, B., Yang, K., Zou, L., and D'Andrea, A.D. (2010). The FANCM/FAAP24 complex is required for the DNA interstrand crosslink-induced checkpoint response. *Mol. Cell* 39, 259–268.
- Huen, M.S., Grant, R., Manke, I., Minn, K., Yu, X., Yaffe, M.B., and Chen, J. (2007). RNF8 transduces the DNA-damage signal via histone ubiquitylation and checkpoint protein assembly. *Cell* 131, 901–914.
- Kim, H., Yang, K., Dejsuphong, D., and D'Andrea, A.D. (2012). Regulation of Rev1 by the Fanconi anemia core complex. *Nat. Struct. Mol. Biol.* 19, 164–170.
- Knipscheer, P., Raschle, M., Smogorzewska, A., Enoiu, M., Ho, T.V., Scharer, O.D., Elledge, S.J., and Walter, J.C. (2009). The Fanconi anemia pathway promotes replication-dependent DNA interstrand cross-link repair. *Science* 326, 1698–1701.
- Kolas, N.K., Chapman, J.R., Nakada, S., Ylanko, J., Chahwan, R., Sweeney, F.D., Panier, S., Mendez, M., Wildenhain, J., Thomson, T.M., et al. (2007). Orchestration of the DNA-damage response by the RNF8 ubiquitin ligase. *Science* 318, 1637–1640.
- Kratz, K., Schopf, B., Kaden, S., Sandoel, A., Eberhard, R., Lademann, C., Cannavo, E., Sartori, A.A., Hengartner, M.O., and Jiricny, J. (2010). Deficiency of FANCD2-associated nuclease KIAA1018/FAN1 sensitizes cells to interstrand crosslinking agents. *Cell* 142, 77–88.
- Leung, J.W., Wang, Y., Fong, K.W., Huen, M.S., Li, L., and Chen, J. (2012). Fanconi anemia (FA) binding protein FAAP20 stabilizes FA complementation group A (FANCA) and participates in interstrand cross-link repair. *Proc. Natl. Acad. Sci. USA* 109, 4491–4496.
- Liu, T., Ghosal, G., Yuan, J., Chen, J., and Huang, J. (2010). FAN1 acts with FANCI-FANCD2 to promote DNA interstrand cross-link repair. *Science* 329, 693–696.
- Lok, G.T., Sy, S.M., Dong, S.S., Ching, Y.P., Tsao, S.W., Thomson, T.M., and Huen, M.S. (2011). Differential regulation of RNF8-mediated Lys48- and Lys63-based poly-ubiquitylation. *Nucleic Acids Res.* 40, 196–205.
- MacKay, C., Declais, A.C., Lundin, C., Agostinho, A., Deans, A.J., MacArtney, T.J., Hofmann, K., Gartner, A., West, S.C., Helleday, T., et al. (2010). Identification of KIAA1018/FAN1, a DNA repair nuclease recruited to DNA damage by monoubiquitinated FANCD2. *Cell* 142, 65–76.
- Mailand, N., Bekker-Jensen, S., Fastrup, H., Melander, F., Bartek, J., Lukas, C., and Lukas, J. (2007). RNF8 ubiquitylates histones at DNA double-strand breaks and promotes assembly of repair proteins. *Cell* 131, 887–900.
- Marteijn, J.A., Bekker-Jensen, S., Mailand, N., Lans, H., Schwertman, P., Gourdin, A.M., Dantuma, N.P., Lukas, J., and Vermeulen, W. (2009). Nucleotide excision repair-induced H2A ubiquitination is dependent on MDC1 and RNF8 and reveals a universal DNA damage response. *J. Cell Biol.* 186, 835–847.
- Meetei, A.R., Sechi, S., Wallisch, M., Yang, D., Young, M.K., Joenje, H., Hoatlin, M.E., and Wang, W. (2003). A multiprotein nuclear complex connects Fanconi anemia and Bloom syndrome. *Mol. Cell Biol.* 23, 3417–3426.
- Muniandy, P.A., Liu, J., Majumdar, A., Liu, S.T., and Seidman, M.M. (2010). DNA interstrand crosslink repair in mammalian cells: step by step. *Crit. Rev. Biochem. Mol. Biol.* 45, 23–49.
- Muniandy, P.A., Thapa, D., Thazhathveetil, A.K., Liu, S.T., and Seidman, M.M. (2009). Repair of laser-localized DNA interstrand cross-links in G1 phase mammalian cells. *J. Biol. Chem.* 284, 27908–27917.
- Nam, E.A., and Cortez, D. (2011). ATR signalling: more than meeting at the fork. *Biochem. J.* 436, 527–536.
- Shen, X., Do, H., Li, Y., Chung, W.-Y., Tomasz, M., de Winter, J.P., Xia, B., Elledge, S.J., Wang, W., and Li, L. (2009). Recruitment of Fanconi anemia and breast cancer proteins to DNA damage sites is differentially governed by replication. *Mol. Cell* 35, 716–723.
- Singh, T.R., Saro, D., Ali, A.M., Zheng, X.F., Du, C.H., Killen, M.W., Sachpatzidis, A., Wahengbam, K., Pierce, A.J., Xiong, Y., et al. (2010). MHF1-MHF2, a histone-fold-containing protein complex, participates in the Fanconi anemia pathway via FANCM. *Mol. Cell* 37, 879–886.
- Smogorzewska, A., Desetty, R., Saito, T.T., Schlabach, M., Lach, F.P., Sowa, M.E., Clark, A.B., Kunkel, T.A., Harper, J.W., Colaiacovo, M.P., et al. (2010). A genetic screen identifies FAN1, a Fanconi anemia-associated nuclease necessary for DNA interstrand crosslink repair. *Mol. Cell* 39, 36–47.
- Sy, S.M., Jiang, J., Dong, S.S., Lok, G.T., Wu, J., Cai, H., Yeung, E.S., Huang, J., Chen, J., Deng, Y., et al. (2011). Critical roles of ring finger protein RNF8 in replication stress responses. *J. Biol. Chem.* 286, 22355–22361.
- Takata, M., Ishiai, M., and Kitao, H. (2009). The Fanconi anemia pathway: insights from somatic cell genetics using DT40 cell line. *Mutat. Res.* 668, 92–102.
- Ulrich, H.D., and Walden, H. (2010). Ubiquitin signalling in DNA replication and repair. *Nat. Rev. Mol. Cell Biol.* 11, 479–489.
- Wang, B., and Elledge, S.J. (2007). Ubc13/Rnf8 ubiquitin ligases control foci formation of the Rap80/Abraxas/Brc1/Brc36 complex in response to DNA damage. *Proc. Natl. Acad. Sci. USA* 104, 20759–20763.
- Wang, W. (2007). Emergence of a DNA-damage response network consisting of Fanconi anaemia and BRCA proteins. *Nat. Rev. Genet.* 8, 735–748.
- Wang, X., Kennedy, R.D., Ray, K., Stuckert, P., Ellenberger, T., and D'Andrea, A.D. (2007). Chk1-mediated phosphorylation of FANCE is required for the Fanconi anemia/BRCA pathway. *Mol. Cell Biol.* 27, 3098–3108.
- Wen, Q., Scora, J., Phear, G., Rodgers, G., Rodgers, S., and Meuth, M. (2008). A mutant allele of MRE11 found in mismatch repair-deficient tumor cells suppresses the cellular response to DNA replication fork stress in a dominant negative manner. *Mol. Biol. Cell* 19, 1693–1705.
- Yamamoto, K.N., Kobayashi, S., Tsuda, M., Kurumizaka, H., Takata, M., Kono, K., Jiricny, J., Takeda, S., and Hirota, K. (2011). Involvement of SLX4 in inter-strand cross-link repair is regulated by the Fanconi anemia pathway. *Proc. Natl. Acad. Sci. USA* 108, 6492–6496.
- Yan, Z., Delannoy, M., Ling, C., Dae, D., Osman, F., Muniandy, P.A., Shen, X., Oostra, A.B., Du, H., Steltenpool, J., et al. (2010). A histone-fold complex and FANCM form a conserved DNA-remodeling complex to maintain genome stability. *Mol. Cell* 37, 865–878.
- Zhao, G.Y., Sonoda, E., Barber, L.J., Oka, H., Murakawa, Y., Yamada, K., Ikura, T., Wang, X., Kobayashi, M., Yamamoto, K., et al. (2007). A critical role for the ubiquitin-conjugating enzyme Ubc13 in initiating homologous recombination. *Mol. Cell* 25, 663–675.

DNA robustly stimulates FANCD2 monoubiquitylation in the complex with FANCI

Koichi Sato¹, Kazue Toda¹, Masamichi Ishiai², Minoru Takata² and Hitoshi Kurumizaka^{1,*}

¹Laboratory of Structural Biology, Graduate School of Advanced Science and Engineering, Waseda University, 2-2 Wakamatsu-cho, Shinjuku-ku, Tokyo 162-8480 and ²Laboratory of DNA Damage Signaling, Radiation Biology Center, Kyoto University, Yoshida-konoe, Sakyo-ku, Kyoto 606-8501, Japan

Received September 28, 2011; Revised January 12, 2012; Accepted January 13, 2012

ABSTRACT

FANCI and FANCD2 form a complex, and play essential roles in the repair of interstrand DNA crosslinks (ICLs) by the Fanconi anemia (FA) pathway. FANCD2 is monoubiquitylated by the FA core complex, composed of 10 FA proteins including FANCL as the catalytic E3 subunit. FANCD2 monoubiquitylation can be reconstituted with purified minimal components, such as FANCI, E1, UBE2T (E2) and FANCL (E3) *in vitro*; however, its efficiency is quite low as compared to the *in vivo* monoubiquitylation of FANCD2. In this study, we found that various forms of DNA, such as single-stranded, double-stranded and branched DNA, robustly stimulated the FANCD2 monoubiquitylation *in vitro* up to a level comparable to its *in vivo* monoubiquitylation. This stimulation of the FANCD2 monoubiquitylation strictly required FANCI, suggesting that FANCD2 monoubiquitylation may occur in the FANCI–FANCD2 complex. A FANCI mutant that was defective in DNA binding was also significantly defective in FANCD2 monoubiquitylation *in vitro*. In the presence of 5' flapped DNA, a DNA substrate mimicking the arrested replication fork, about 70% of the input FANCD2 was monoubiquitylated, while less than 1% FANCD2 monoubiquitylation was observed in the absence of the DNA. Therefore, DNA may be the unidentified factor required for proper FANCD2 monoubiquitylation.

INTRODUCTION

Fanconi anemia (FA) is an autosomal recessive disorder, and 15 FA genes, *FANCA*, *-B*, *-C*, *-D1* (*BRCA2*), *-D2*,

-E, *-F*, *-G*, *-I*, *-J* (*BRIP1*), *-L*, *-M*, *-N* (*PALB2*), *-O* (*RAD51C*) and *-P* (*SLX4*), have been identified (1–3). In FA patients, mutations in these FA genes cause genomic instability with cancer susceptibility, progressive bone marrow failure and multiple developmental defects (1–4). These FA gene products are considered to function in a common DNA damage repair pathway, the 'FA pathway'.

In the FA pathway, eight proteins, FANCA, FANCB, FANCC, FANCE, FANCF, FANCG, FANCL and FANCM, and two FANCA-associated polypeptides (FAAPs) form the FA core complex, and FANCI and FANCD2 form the ID complex (5–8). When cells are exposed to DNA crosslinking agents, the ID complex promptly becomes monoubiquitylated (6–9). This monoubiquitylation of the ID complex, especially for FANCD2, is a central process in the FA pathway, and the FA core complex is responsible for it, as the E3 ubiquitin ligase complex (5,9–11). FANCL was identified as the catalytic E3 subunit for the FANCD2 monoubiquitylation by the FA core complex (12). On the other hand, UBE2T, which is required for cellular resistance to interstrand DNA crosslinks (ICLs), has been shown to interact with FANCL, and functions as the E2 ubiquitin-conjugating enzyme required for the FANCL-dependent FANCD2 monoubiquitylation (13). An *in vitro* study showed that E1, UBE2T, and FANCL are sufficient for FANCD2 monoubiquitylation (14). However, the efficiency of FANCD2 monoubiquitylation is extremely low, as compared to that of FANCD2 monoubiquitylation during ICL repair *in vivo* (9). Therefore, an essential factor(s) required for mediating FANCD2 monoubiquitylation is missing in the *in vitro* FANCD2 monoubiquitylation assay.

In the present study, we prepared the ID complex with recombinant FANCI and FANCD2, and performed *in vitro* monoubiquitylation assays with recombinant E1, UBE2T (E2) and FANCL (E3). We found that FANCD2

*To whom correspondence should be addressed. Tel: +81 3 5369 7315; Fax: +81 3 5367 2820; Email: kurumizaka@waseda.jp

The authors wish it to be known that, in their opinion, the first two authors should be regarded as Joint First Authors.

© The Author(s) 2012. Published by Oxford University Press.

This is an Open Access article distributed under the terms of the Creative Commons Attribution Non-Commercial License (<http://creativecommons.org/licenses/by-nc/3.0>), which permits unrestricted non-commercial use, distribution, and reproduction in any medium, provided the original work is properly cited.

monoubiquitylation in the ID complex was robustly stimulated by DNA, such as single-stranded, double-stranded and branched DNAs, up to the level comparable to the *in vivo* monoubiquitylation of FANCD2.

MATERIALS AND METHODS

Purification of chicken FANCD2, FANCI, FANCL and human UBE2T

The DNA fragments encoding chicken FANCD2 and FANCI were ligated into the *NdeI*-*BamHI* and *NdeI*-*XhoI* sites of the pET-15b vector, respectively, and the proteins were overexpressed in the *Escherichia coli* BL21(DE3) strain, which also carried an expression vector for the minor tRNAs [Codon(+)-RIL, Stratagene]. The cells were cultured in LB medium supplemented with ampicillin (100 µg/ml) and chloramphenicol (35 µg/ml) at 30°C to an OD₆₀₀ = 0.6, and then protein production was induced by adding 0.5 mM Isopropyl β-D-1-thiogalactopyranoside and culturing the cells overnight at 18°C. The cells were collected, resuspended in buffer A containing 50 mM Tris-HCl (pH 8.0), 10% glycerol, 0.5 M NaCl, 1 mM PMSF, 12 mM imidazole and 5 mM 2-mercaptoethanol, and disrupted by sonication. After disruption, the supernatant was separated from the cell debris by centrifugation (27 200g) at 4°C for 20 min, and was mixed gently with nickel-nitrilotriacetic acid (Ni-NTA) agarose resin (3 ml; Qiagen) at 4°C for 1 h. Later, the Ni-NTA beads were packed into an Econo-Column (Bio-Rad), and were washed with 150 ml buffer A. His₆-tagged FANCD2 or FANCI was eluted with a 60 ml linear gradient of 12 to 400 mM imidazole in buffer A. Since the His₆-tag may affect the DNA-binding property of the proteins, the His₆-tag was removed by digestion with thrombin protease (GE Healthcare; 3 U/mg protein for FANCD2, 20 U/mg protein for FANCI) during dialysis against 4 L of buffer B, containing 20 mM Tris-HCl (pH 8.0), 10% glycerol, 5 mM 2-mercaptoethanol and 0.2 M NaCl. After removal of the His₆-tag, the protein solutions were then loaded onto a Heparin Sepharose CL-6B column (3 ml; GE Healthcare) equilibrated with buffer B. The column was washed with 150 ml of buffer B containing 280 mM NaCl, and the proteins were eluted with a 60 ml linear gradient of 280 to 1000 mM NaCl in buffer B. Peak fractions were collected, concentrated and then applied to a Superdex 200 gel filtration column (HiLoad 26/60 preparation grade; GE Healthcare) equilibrated with buffer B. Purified proteins were concentrated to 5 mg/ml, and were stored at -80°C. All of the FANCI and FANCD2 mutants, except for FANCI Ex6, were purified by the same method as that used for the wild-type FANCI or FANCD2 protein. For the FANCI Ex6 mutant purification, Q Sepharose Fast Flow column chromatography (3 ml; GE Healthcare) was employed, instead of Heparin Sepharose column chromatography. The column was washed with 100 ml of buffer B containing 215 mM NaCl, and the proteins were eluted with a 60 mL linear gradient of 215–450 mM NaCl in buffer B.

The subsequent purification procedure for FANCI Ex6 was the same as that for the wild-type FANCI.

The DNA fragments encoding chicken FANCL and human UBE2T were each ligated separately into the *EcoRI*-*XhoI* sites of the pGEX6P-1 vector, and the proteins were expressed by the same methods as for chicken FANCD2 and FANCI. The cells producing FANCL or UBE2T were collected, resuspended in buffer C, containing 50 mM Tris-HCl (pH 8.0), 10% glycerol, 0.5 M NaCl, 1 mM PMSF, 1 mM EDTA, 0.1% Nonidet P-40 and 5 mM 2-mercaptoethanol, and disrupted by sonication. After disruption, the supernatant was separated from the cell debris by centrifugation for 30 min, and was then mixed gently with Glutathione Sepharose 4B beads (3 ml; GE Healthcare) at 4°C for 2 h. The Glutathione Sepharose 4B beads were packed into an Econo-Column, and were washed with 150 ml of buffer C containing 1 M NaCl. The GST-tagged FANCL or UBE2T was eluted with 50 ml of buffer C containing 20 mM reduced glutathione. Peak fractions were collected, concentrated and then applied to a Superdex 200 gel filtration column equilibrated with buffer B containing 150 mM NaCl. Purified GST-FANCL was concentrated to 3 mg/ml, and was stored at -80°C. The GST-tag of the GST-UBE2T was removed by an overnight treatment with PreScission protease (GE Healthcare; 1.5 U/mg protein) at 4°C. After the GST-tag removal, the protein solution was mixed gently with Glutathione Sepharose 4B at 4°C for 3 h. The flow-through fractions containing purified UBE2T were collected, concentrated to 3 mg/ml, and stored at -80°C. The protein concentration was determined by the Bradford method (15), using bovine serum albumin as the standard protein.

DNA substrates

49-mer single-stranded oligonucleotides, 1, 2, 3 and 4, (16–18) with the sequences 5'-ATCGA TGTCT CTAGA CAGCT GCTCA GGATT GATCT GTAAT GGCCT GGGA-3', 5'-GTCCC AGGCC ATTAC AGATC AAT CC TGAGC ATGTT TACCA AGCGC ATTG-3', 5'-TG ATC ACTTG CTAGC GTCGC AATCC TGAGC AGC TG TCTAG AGACA TCGA-3' and 5'-CCAAT GCGCT TGGTA AACAT GCTCA GGATT GCGAC GCTAG C AAGT GATC-3', respectively, were used to prepare the synthetic Holliday junction (HJ) (1, 2, 3 and 4) by annealing. The splayed arm DNA was prepared by annealing oligonucleotides 1 and 2. The dsDNA was prepared by annealing oligonucleotide 1 with its complementary oligonucleotide. The 5' flapped DNA was prepared by annealing 5'-CAATGCGCTTGGTAAACA-3' to the 3' ssDNA region of the splayed arm DNA. The static fork DNA was prepared by annealing 5'-GCTGTCTAGAGA CATCGAT-3' to the 5' ssDNA region of the 5' flapped DNA. All of the oligonucleotides were purified by HPLC, and the DNA concentrations are expressed in moles of nucleotides.

DNA binding assay

The synthetic HJ (4.5 µM), splayed arm DNA (4.5 µM), and dsDNA (4.5 µM) were mixed with 0.05–0.20 µM of

the ID complex in 10 μ L of reaction buffer, containing 20 mM Tris-HCl (pH 8.0), 70 mM NaCl, 2% glycerol, 0.3 mM MgCl₂, 5 mM dithiothreitol and 10 μ g/ml bovine serum albumin. For the experiments with three-way branched DNAs, splayed arm DNA (4.5 μ M), 5' flapped DNA (4.5 μ M) and static fork DNA (4.5 μ M) were mixed with 0.05–0.20 μ M of the ID complex in 10 μ L of reaction buffer. The samples were incubated at 37°C for 15 min, and were then analyzed by 8.0% or 3.5% PAGE in TBE (18 mM Tris-borate and 0.4 mM EDTA) buffer. DNAs were visualized by SYBR Gold (Invitrogen) staining.

In vitro ubiquitylation assay

The purified FANCD2 protein (1 μ M) or the ID complex (1 μ M) was mixed with UBE2T (2–8 μ M), GST-FANCL (2 μ M), human recombinant E1 (75 nM) (Boston Biochem) and HA-tagged ubiquitin (10 μ M) (Boston Biochem), in the presence or absence of DNA substrates, in 20 μ L of reaction buffer, containing 0.5 mM DTT, 2 mM ATP, 2 mM MgCl₂, 50 mM Tris-HCl (pH 7.5), 3.6% glycerol and 64 mM NaCl. The reactions were incubated for 90 min at 30°C, and were then stopped by the addition of 2% sodium dodecyl sulphate. The reaction products were separated by 7% sodium dodecyl sulphate-polyacrylamide gel electrophoresis (SDS-PAGE), and were transferred to a polyvinylidene fluoride membrane. Ubiquitylated proteins were detected by an anti-HA antibody (F-7; Santa Cruz Biotechnology, Inc.), and protein bands were visualized by Coomassie Brilliant Blue staining.

RESULTS

In vitro monoubiquitylation of the FANCI-FANCD2 complex

Chicken FANCI and FANCD2 were purified as recombinant proteins (Figure 1A, lanes 2 and 4), and the ID complex was prepared by mixing them in 1:1 stoichiometry. We also purified UBE2T and FANCL, which are known as the E2 and E3 proteins for FANCD2 monoubiquitylation, respectively, as recombinant proteins (Figure 1B and C). We then performed the *in vitro* monoubiquitylation assay (14). The ID complex was incubated with E1, UBE2T and FANCL in the presence of HA-tagged ubiquitin (Figure 2A), and the ubiquitylated proteins were detected by a western blotting analysis with an anti-HA antibody (Figure 2B).

As shown in Figure 2B, FANCD2 was monoubiquitylated in this assay (lane 6). The FANCD2 K563R mutant, which is defective in monoubiquitylation *in vivo* (9), was also defective in this monoubiquitylation assay (Figure 2B, lane 7), suggesting that the FANCD2 monoubiquitylation properly occurred in this *in vitro* system. The FANCD2 monoubiquitylation may predominantly occur in the ID complex, because only a background level of FANCD2 monoubiquitylation was observed in the absence of FANCI (Figure 2B, lanes 2 and 3). Consistently, FANCD2 monoubiquitylation was not stimulated when the chicken FANCI R1288Q mutant, corresponding to the human FANCI R1285Q mutant,

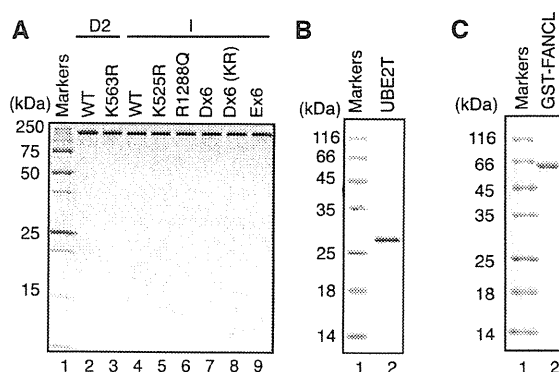


Figure 1. Purification of chicken FANCD2, FANCI, FANCL and human UBE2T. (A) Purified chicken FANCD2 and FANCI, used for *in vitro* assays, were analyzed by 15% SDS-PAGE with Coomassie Brilliant Blue staining. Lane 1 indicates the molecular mass markers. Lanes 2 and 3 indicate purified FANCD2 and FANCD2 K563R, respectively. Lanes 4–9 indicate purified FANCI, FANCI K525R, FANCI R1288Q, FANCI Dx6, FANCI Dx6 K525R and FANCI Ex6, respectively. (B) Purified human UBE2T, used for *in vitro* monoubiquitylation assays, was analyzed by 15% SDS-PAGE with Coomassie Brilliant Blue staining. Lane 1 indicates the molecular mass markers. Lane 2 indicates purified UBE2T. (C) Purified GST-tagged chicken FANCL, used for *in vitro* monoubiquitylation assays, was analyzed by 15% SDS-PAGE with Coomassie Brilliant Blue staining. Lane 1 indicates the molecular mass markers. Lane 2 indicates purified GST-tagged FANCL.

which is reportedly defective in both FANCD2 and DNA binding (19), was added instead of FANCI (Figure 2C, lane 7). Interestingly, the FANCI K525R mutant, which is defective in FANCI monoubiquitylation *in vivo*, was proficient in stimulating FANCD2 monoubiquitylation *in vitro* (Figure 2B, lane 8). In our *in vitro* system, FANCI monoubiquitylation was weakly observed in the presence of FANCD2 (Figure 2B, lane 6). However, the weak FANCI monoubiquitylation observed in the ID complex may not properly occur on the Lys525 residue of FANCI, for the following reasons. First, this weak monoubiquitylation was also observed with the FANCI K525R mutant (Figure 2B, lanes 8 and 9). Second, the FANCI monoubiquitylation occurred on the Lys525 residue without FANCD2 (Figure 2B, lane 4), as previously reported (20), but the weakly monoubiquitylated FANCI in the ID complex migrated slightly faster than the Lys525-monoubiquitylated FANCI (Figure 2B, lane 4 versus lane 6).

DNAs robustly stimulate FANCD2 monoubiquitylation

Upon the induction of DNA crosslinking damage, 40–70% of FANCD2 was reportedly monoubiquitylated in cells (11,21). However, we observed less than 1% monoubiquitylation of the input FANCD2 *in vitro* (Figure 2D). This indicated that an essential component required for the proper monoubiquitylation of FANCD2 was missing in this *in vitro* system. The FANCD2 monoubiquitylation site is reportedly buried in the binding interface with FANCI in the ID complex (22). Interestingly, the putative DNA-binding path in the ID

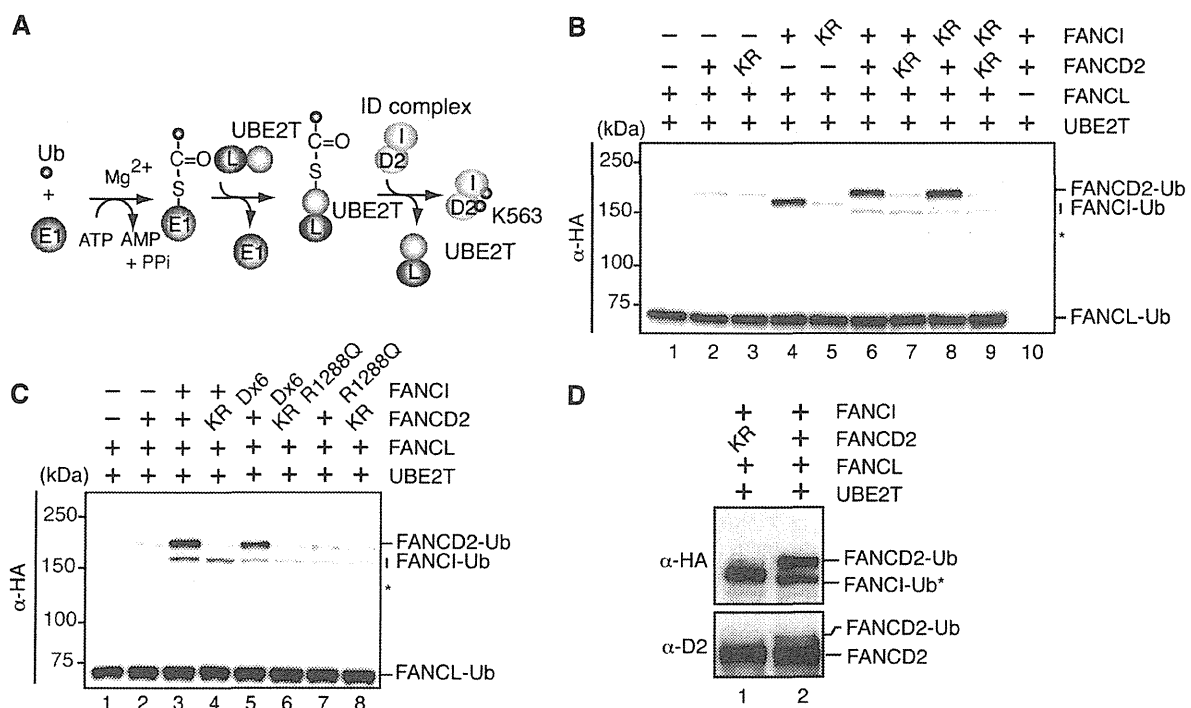


Figure 2. *In vitro* monoubiquitylation of FANCD2. (A) Schematic diagram of the monoubiquitylation assay. The monoubiquitylation assay was performed by incubating FANCD2 (D2) or FANCI (I)-FANCD2 with E1, UBE2T and FANCL (L) in the presence of ATP and HA-tagged ubiquitin (Ub). (B) Ubiquitylated proteins were separated by 7% SDS-PAGE, and were detected by western blotting with an anti-HA monoclonal antibody (α -HA). Lanes 1 and 2 indicate control experiments without FANCI-FANCD2 and FANCI, respectively. Lane 3 indicates an experiment with FANCD2 K563R in the absence of FANCI. Lane 4 indicates an experiment with FANCI in the absence of FANCD2. Lane 5 indicates an experiment with FANCI K525R in the absence of FANCD2. Lane 6 indicates an experiment in the presence of the complete set of proteins. Lane 7 indicates an experiment with FANCD2 K563R, in the presence of FANCI. Lane 8 indicates an experiment with FANCI K525R, in the presence of FANCD2. Lane 9 indicates an experiment with FANCD2 K563R and FANCI K525R. Lane 10 indicates an experiment with FANCD2 and FANCI, without FANCL. Asterisk indicates the degradation product of monoubiquitylated FANCI. (C) Experiments were performed as in panel (B). Lanes 1 and 2 indicate control experiments without FANCI-FANCD2 and FANCI, respectively. Lane 3 indicates an experiment in the presence of the complete set of proteins. Lane 4 indicates an experiment with FANCD2 K563R, in the presence of FANCI. Lanes 5 and 6 indicate experiments with FANCI Dx6, in the presence of FANCD2 and FANCD2 K563R, respectively. Lanes 7 and 8 indicate experiments with FANCI R1288Q, in the presence of FANCD2 and FANCD2 K563R, respectively. Asterisk indicates the degradation product of monoubiquitylated FANCI. (D) Experiments were performed as in panel (B). Enlarged images of the monoubiquitylated FANCD2 band detected by α -HA (upper panel) and an anti-chicken FANCD2 polyclonal antibody (lower panel). FANCI-Ub* indicates non-specific monoubiquitylation of FANCI. Lane 1 indicates a negative control experiment in the presence of FANCD2 K563R. Lane 2 indicates an experiment in the presence of the complete set of proteins.

complex is located near the FANCD2 monoubiquitylation site (22). This suggested that DNA binding by the ID complex may induce a conformational change of the ID complex, and may expose the FANCD2 monoubiquitylation site on an accessible surface.

We therefore tested whether the DNA affected the FANCD2 monoubiquitylation in the ID complex *in vitro*. We tested seven DNA structures, including splayed arm DNA, 5' flapped DNA, 3' flapped DNA, static fork DNA, HJ DNA, ssDNA and dsDNA, as substrates (Figure 3A). To our surprise, we found that the FANCD2 monoubiquitylation in the ID complex was robustly enhanced in the presence of these DNAs (Figure 3B). This FANCD2 monoubiquitylation stimulation by DNA was not observed in the absence of FANCI (Figure 3B, lanes 1–4) or in the presence of the FANCD2 K563R mutant, instead of FANCD2 (Figure 3B, lanes 5, 10, 15, 20, 25, 30, 35 and 40). The ID complex bound to the 5' flapped DNA, but E1, UBE2T and FANCL did not

(Figure 3C). Therefore, we conclude that DNA binding by the ID complex is required for the robust stimulation of the FANCD2 monoubiquitylation. Since about 70% of FANCD2 was monoubiquitylated after a 6 h reaction in the presence of FANCI and 5' flapped DNA, the FANCD2 monoubiquitylation can be promoted to the level observed in cells with DNA and FANCI *in vitro* (Figure 3D).

The FANCI R1288Q mutant is defective in stimulating FANCD2 monoubiquitylation

The human FANCI R1285Q mutant, corresponding to the chicken FANCI R1288Q mutant, is reportedly defective in both FANCD2 binding and DNA binding (19). We found that the FANCI R1288Q mutant was significantly defective in stimulating the FANCD2 monoubiquitylation in the presence of DNA *in vitro* (Figure 3E, lanes 6–10). The DNA-binding activity of FANCI alone was consistent with that reported previously

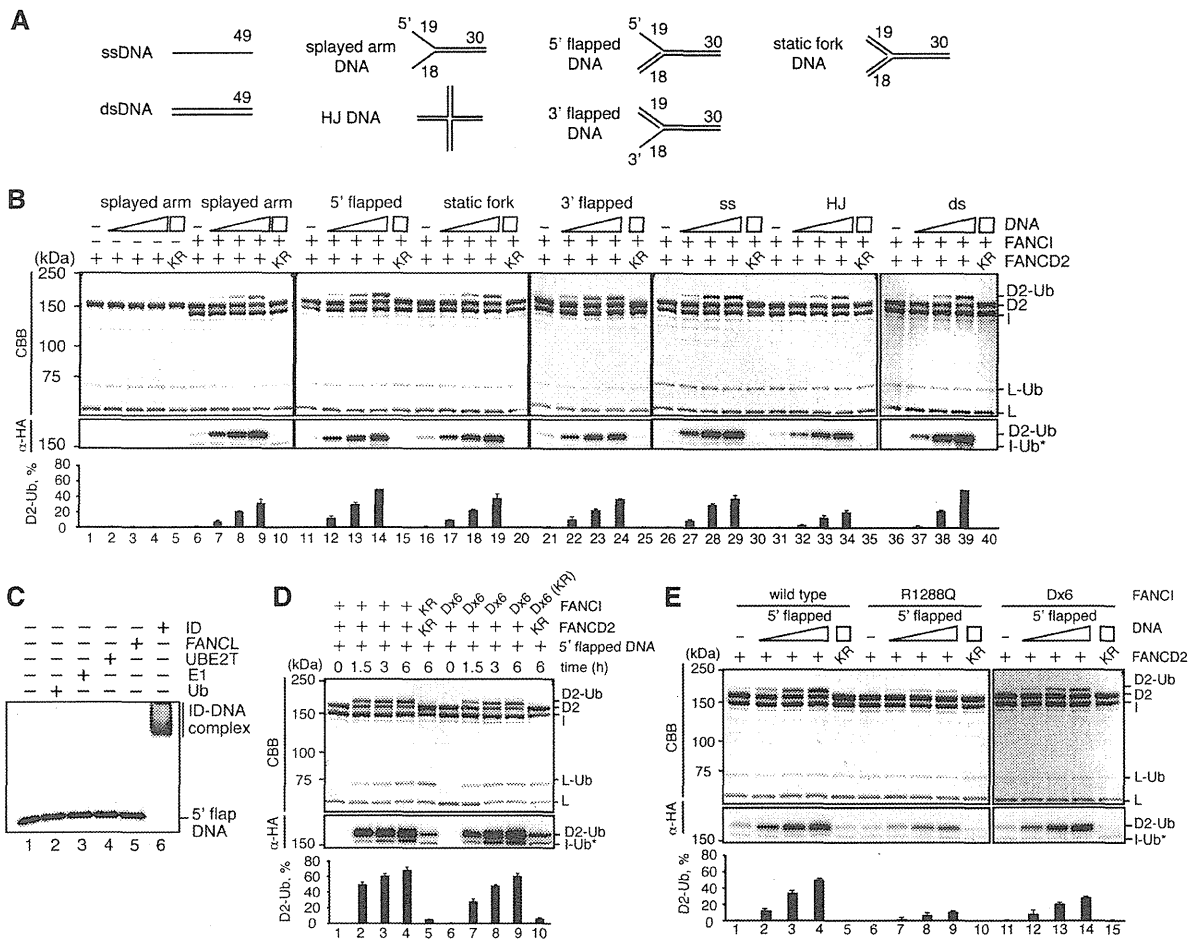


Figure 3. DNA stimulates FANCD2 monoubiquitylation *in vitro*. (A) Schematic representation of the DNA substrates. (B) FANCD2 (lanes 1–4) or FANCI–FANCD2 (lanes 6–9, 11–14, 16–19, 21–24, 26–29, 31–34 and 36–39) was incubated with E1, UBE2T and FANCL in the presence of ATP and HA-tagged ubiquitin. The reactions were performed in the presence of splayed arm DNA (lanes 2–5 and 6–10), 5' flapped DNA (lanes 12–15), static fork DNA (lanes 17–20), 3' flapped DNA (lanes 22–25), ssDNA (lanes 27–30), HJ DNA (lanes 32–35), and dsDNA (lanes 37–40). The DNA concentrations were 0 μ M (lanes 1, 6, 11, 16, 21, 26, 31 and 36), 5 μ M (lanes 2, 7, 12, 17, 22, 27, 32 and 37), 20 μ M (lanes 3, 8, 13, 18, 23, 28, 33 and 38), and 50 μ M (lanes 4, 5, 9, 10, 14, 15, 19, 20, 24, 25, 29, 30, 34, 35, 39 and 40). Lanes 5, 10, 15, 20, 25, 30, 35 and 40 indicate negative control experiments with FANCD2 K563R. Proteins were separated by 7% SDS-PAGE, blotted onto a membrane, and detected by Coomassie Brilliant Blue staining (upper panel) or α -HA antibody staining (middle panel). The amounts of monoubiquitylated FANCD2 were estimated, and the averages of three independent experiments are indicated as black bars with the standard deviation values (lower panel). (C) Gel shift assay. 5' flapped DNA (5 μ M) was incubated with ubiquitin (10 μ M) (lane 2), E1 (75 nM) (lane 3), UBE2T (2 μ M) (lane 4), GST-FANCL (2 μ M) (lane 5), or FANCI–FANCD2 (1 μ M) (lane 6) at 30°C for 15 min. Samples were analyzed by 3.5% PAGE in 0.2 \times TBE buffer (18 mM Tris base, 18 mM boric acid, and 0.4 mM EDTA) with SYBR Gold staining. (D) Time course experiments of the FANCD2 monoubiquitylation. Experiments were performed as in panel (B). FANCI–FANCD2 (lanes 1–4) or FANCI Dx6–FANCD2 (lanes 6–9) was incubated with 50 μ M 5' flapped DNA. Reaction times were 0 h (lanes 1 and 6), 1.5 h (lanes 2 and 7), 3 h (lanes 3 and 8) and 6 h (lanes 4, 5, 9 and 10). Lanes 5 and 10 indicate negative control experiments with FANCD2 K563R and FANCI K525R or FANCI Dx6 K525R, respectively. The results are presented as in panel B. (E) The stimulation of FANCD2 monoubiquitylation by FANCI R1288Q and FANCI Dx6. Experiments were performed as in panel (B), with 5' flapped DNA and FANCI R1288Q (lanes 6–10) or FANCI Dx6 (lanes 11–15), instead of FANCI (lanes 1–5). The DNA concentrations were 0 μ M (lanes 1, 6 and 11), 5 μ M (lanes 2, 7 and 12), 20 μ M (lanes 3, 8 and 13), and 50 μ M (lanes 4, 5, 9, 10, 14 and 15). Lanes 5, 10 and 15 indicate negative control experiments with FANCD2 K563R.

(20), in which FANCI preferentially binds to the HJ DNA (Figure 4A and B). The FANCI R1288Q mutant alone was proficient in the DNA binding (Figure 4A and B), unlike the human FANCI R1285Q mutant (19); however, the DNA-binding activity of the ID complex containing the FANCI R1288Q mutant was clearly reduced (Figure 4C and D), as compared to the wild-type ID complex (Figure 4C and D). Therefore, both the FANCD2-binding and DNA-binding activities

of FANCI may be required for stimulating the FANCD2 monoubiquitylation.

The FANCI Dx6 mutant stimulates FANCD2 monoubiquitylation at a reduced rate

The FANCI Dx6 mutant, in which Ser558, Ser561, Thr567, Ser598, Ser619 and Ser631 are replaced by Asp, reportedly induces constitutive FANCD2

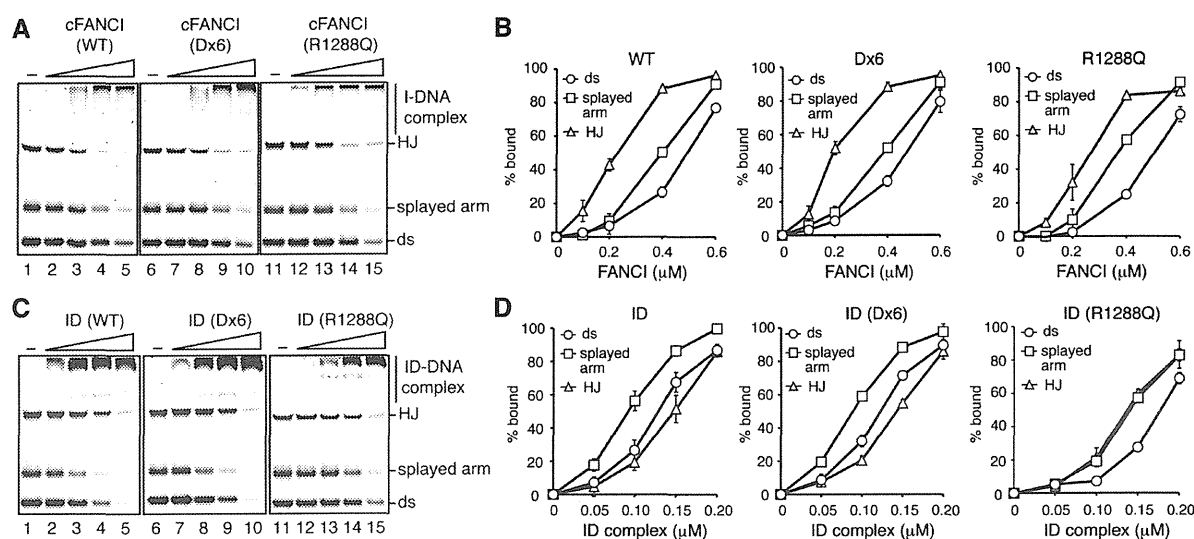


Figure 4. DNA binding activities of the ID complex and FANCI. (A) Competitive DNA-binding assay with FANCI. The synthetic HJ DNA (4.5 μ M), splayed arm DNA (4.5 μ M), and dsDNA (4.5 μ M) were incubated with increasing amounts (0, 0.1, 0.2, 0.4 and 0.6 μ M) of FANCI (lanes 1–5), FANCI Dx6 (lanes 6–10), or FANCI R1288Q (lanes 11–15) at 37°C for 15 min. The samples were then separated by 8% PAGE in 0.2 \times TBE buffer, and the bands were visualized by SYBR Gold staining. (B) Graphic representations of the experiments with FANCI (left), FANCI Dx6 (center), and FANCI R1288Q (right) shown in panel (A). The DNAs bound to FANCI were estimated, and the averages of three independent experiments are plotted against the protein concentrations with the standard deviation values. (C) Competitive DNA-binding assay with the ID complex. Experiments were performed as in panel (B). The FANCI–FANCD2 (lanes 1–5), FANCI Dx6–FANCD2 (lanes 6–10), and FANCI R1288Q–FANCD2 (lanes 11–15) concentrations were 0, 0.05, 0.10, 0.15 and 0.20 μ M. (D) Graphic representations of the experiments with FANCI–FANCD2 (left), FANCI Dx6–FANCD2 (center), and FANCI R1288Q–FANCD2 (right) shown in panel (C). The DNAs bound to the ID complex were estimated, and the averages of three independent experiments are plotted against the protein concentrations with the standard deviation values.

monoubiquitylation *in vivo* (11). We found that the FANCI Dx6 mutant also supported the stimulation of the FANCD2 monoubiquitylation in the presence or absence of DNA, at a reduced rate as compared to FANCI (Figure 2C, lane 5, and Figure 3E, lanes 11–15). The FANCD2 monoubiquitylation stimulation by the FANCI Dx6 mutant was still significant, because about 55% of the FANCD2 was monoubiquitylated in the ID complex containing the FANCI Dx6 mutant during the 6 h reaction in the presence of 5' flapped DNA (Figure 3D). These results are consistent with the previous *in vivo* results, in which the FANCD2 monoubiquitylation in the DT40 cells harboring the FANCI Dx6 mutant occurs at a slightly reduced rate, as compared to the wild-type cells, in the presence of mitomycin C (11). The FANCI Dx6 mutant alone and the ID complex containing the FANCI Dx6 mutant were completely proficient in DNA binding (Figure 4). Therefore, the FANCI phosphorylation mimicked by the FANCI Dx6 mutation may not significantly affect the DNA-binding and FANCI–FANCD2-binding activities of FANCI, although the mechanism of the constitutive FANCD2 monoubiquitylation by the FANCI Dx6 mutant in the absence of DNA damage remains unknown (11).

The DNA-binding activity of FANCI is required to stimulate FANCD2 monoubiquitylation

Finally, we tested whether the DNA-binding activity of FANCI is required to stimulate FANCD2

monoubiquitylation *in vitro*. To do so, we designed the FANCI Ex6 mutant, in which Lys293, Lys296, Lys305, Lys333, Arg338 and Lys341 were replaced by Glu. These amino acid residues are located near the DNA-binding surface of FANCI (22). As anticipated, the FANCI Ex6 mutant alone and the ID complex containing the FANCI Ex6 mutant were significantly defective in DNA binding (Figure 5A–D). Interestingly, the FANCI Ex6 mutant was also quite defective in the DNA-stimulated FANCD2 monoubiquitylation *in vitro* (Figure 5F). In the absence of DNA, the FANCI Ex6 mutant induced the FANCD2 monoubiquitylation as well as FANCI (Figure 5E), indicating the proficiency of FANCD2 binding by the FANCI Ex6 mutant. These results strongly suggested that the DNA-binding activity of FANCI plays an essential role in the DNA-stimulated FANCD2 monoubiquitylation.

DISCUSSION

Monoubiquitylation of FANCD2 is the central process for DNA crosslink repair by the FA pathway. FANCL has been identified as a catalytic component of the E3 ligase FA core complex, containing FANCA, –B, –C, –E, –F, –G, –L, –M and two FANCA-associated polypeptides (FAAPs). UBE2T has been identified as an E2 ubiquitin-conjugating enzyme for the FANCD2 monoubiquitylation (13). Alpi *et al.* (14) successfully reconstituted the FANCD2 monoubiquitylation *in vitro*

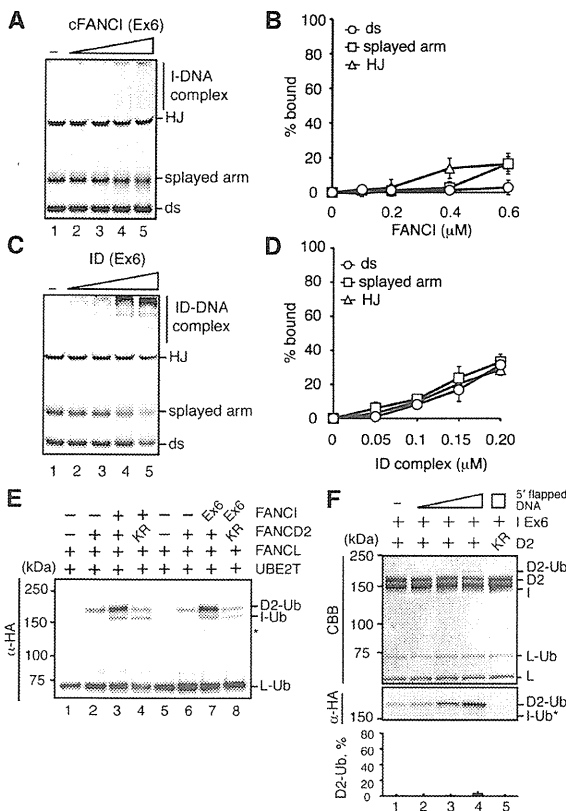


Figure 5. The DNA-binding activity of FANCI is required for robust stimulation of the FANCD2 monoubiquitylation. (A) Competitive DNA-binding assay with FANCI Ex6. Experiments were performed as in Figure 4A. (B) Graphic representation of the experiments shown in panel (A). The DNAs bound to FANCI Ex6 were estimated, and the averages of three independent experiments are plotted against the protein concentrations with the standard deviation values. (C) Competitive DNA-binding assay with FANCI Ex6-FANCD2. Experiments were performed as in Figure 4C. (D) Graphic representation of the experiments shown in panel (C). The DNAs bound to the ID (Ex6) complex were estimated, and the averages of three independent experiments are plotted against the protein concentrations with the standard deviation values. (E) *In vitro* monoubiquitylation assay with FANCI Ex6 in the absence of DNA. Proteins were separated by 7% SDS-PAGE, blotted onto a membrane, and detected by α -HA antibody staining. (F) *In vitro* monoubiquitylation assay with FANCI Ex6 in the presence of 5' flapped DNA. Experiments were performed as in Figure 3E. Proteins were separated by 7% SDS-PAGE, blotted onto a membrane and detected by Coomassie Brilliant Blue staining (upper panel) or α -HA antibody staining (middle panel). The amounts of monoubiquitylated FANCD2 were estimated, and the averages of three independent experiments are indicated as black bars with the standard deviation values (lower panel).

with purified UBE2T and FANCL, and in the present study, we also observed the *in vitro* FANCD2 monoubiquitylation in the ID complex with purified E1, UBE2T and FANCL. However, only slight FANCD2 monoubiquitylation (less than 1% of the input FANCD2) was detected *in vitro*, although robust FANCD2 monoubiquitylation (40–70%) has been detected *in vivo* (11,21). These results, therefore, indicated that the factor(s) required for proper FANCD2

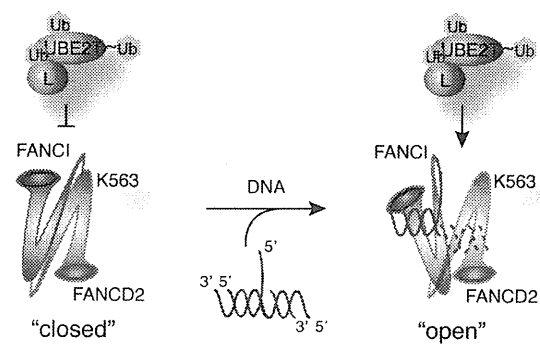


Figure 6. Model for the role of branched DNA in FANCD2 monoubiquitylation. According to the crystal structure of the ID complex (22), the monoubiquitylation site (K563) of FANCD2 is located near the interface with FANCI. Therefore, UBE2T and FANCL may not allow access to the FANCD2 monoubiquitylation site in the ID complex (left panel). Branched DNA may bind to FANCI, as revealed by the crystal structure of the FANCI-DNA complex (22), and thus induce a conformational change of the ID complex to expose the FANCD2 monoubiquitylation site for UBE2T and FANCL (right panel).

monoubiquitylation may be missing in the *in vitro* FANCD2 monoubiquitylation system.

The crystal structure of the ID complex was recently reported (22). In the ID complex structure, however, the monoubiquitylation site of FANCD2 is buried in the FANCI-FANCD2 interface. This raises a new question: How does the ubiquitin ligase gain access to its target sites on the ID complex? This may be explained if a conformational change of the ID complex occurs upon DNA binding, thus relocating the FANCD2 monoubiquitylation site on the accessible surface of the complex. Since the three-way branched DNA is predicted to bind near the FANCD2 monoubiquitylation site in the ID complex (22), it may induce such a conformational change of the ID complex when it binds (Figure 6).

Consistent with the idea described above, in the present study, we found that DNA robustly stimulates the FANCD2 monoubiquitylation, up to a level comparable to the *in vivo* FANCD2 monoubiquitylation. This is consistent with the previous observation that DNA fragments trigger FANCD2 monoubiquitylation in crude *Xenopus laevis* egg extracts (23). It has been proposed that the FA core complex monoubiquitylates FANCD2, and that its monoubiquitylation is required to recruit the ID complex to chromatin (10,24). However, our findings suggested that FANCD2 monoubiquitylation may occur after it binds to the damaged DNA. This discrepancy may be explained, if the FA core complex is considered to function in the chromatin targeting of the ID complex, and then the FANCD2 monoubiquitylation occurs after its chromatin targeting. The FA core complex has been proposed to have multiple functions within the FA pathway (10), and thus the ID complex recruitment to chromatin may be one of them. Alternatively, monoubiquitylation of the ID complex by the FA core complex in chromatin may prevent the dissociation of the ID complex from the damaged chromatin. This idea

is consistent with the previous observation that the FANCD2 K563R mutant, which was defective in its monoubiquitylation, did not stably associate with chromatin (10).

Monoubiquitylated FANCD2 in chromatin is proposed to function in recruiting ubiquitin-binding proteins, such as FAN1 and SLX4, to chromatin (1,25). FAN1 is the Fanconi anemia associated nuclease, which is considered to promote nucleolytic incisions of the crosslink and/or the processing of HR intermediates (26–29). SLX4 is considered to function as a scaffold that interacts with the other nucleases, SLX1, XPF and MUS81 (30–32). The DNA-stimulated monoubiquitylation of FANCD2 reported here may occur just before the recruitment of these nucleases required for DNA crosslink repair.

In the present *in vitro* assay, unlike FANCD2, FANCI was not properly monoubiquitylated in the ID complex, although the FANCD2-free FANCI was properly monoubiquitylated. This may suggest that the essential factor(s) for FANCI monoubiquitylation in the ID complex is still missing in this system. The subunits of the FA core complex may be potential candidates for the factor required for proper monoubiquitylation of FANCI in the ID complex. The development of an *in vitro* system for FANCI monoubiquitylation in the ID complex will be needed to evaluate the significance of the monoubiquitylations of both FANCI and FANCD2.

FUNDING

This work was supported in part by Grants-in-Aid from the Japanese Society for the Promotion of Science (JSPS), and the Ministry of Education, Culture, Sports, Science and Technology (MEXT), Japan. Waseda Research Institute for Science and Engineering (to H.K.). Ichiro Kanehara Foundation and the Mochida Memorial Foundation for Medical and Pharmaceutical Research (to M.I.). Funding for open access charge: Waseda University.

Conflict of interest statement. None declared.

REFERENCES

- Garner,E. and Smogorzewska,A. (2011) Ubiquitylation and the Fanconi anemia pathway. *FEBS Lett.*, **585**, 2853–2860.
- Kee,Y. and D'Andrea,A.D. (2010) Expanded roles of the Fanconi anemia pathway in preserving genomic stability. *Genes Dev.*, **24**, 1680–1694.
- Kitao,H. and Takata,M. (2011) Fanconi anemia: a disorder defective in the DNA damage response. *Int. J. Hematol.*, **93**, 417–424.
- Auerbach,A.D. (2009) Fanconi anemia and its diagnosis. *Mutat. Res.*, **668**, 4–10.
- Wang,W. (2007) Emergence of a DNA-damage response network consisting of Fanconi anaemia and BRCA proteins. *Nat. Rev. Genet.*, **8**, 735–748.
- Smogorzewska,A., Matsuoka,S., Vinciguerra,P., McDonald,E.R. 3rd., Hurov,K.E., Luo,J., Ballif,B.A., Gygi,S.P., Hofmann,K., D'Andrea,A.D. *et al.* (2007) Identification of the FANCI protein, a monoubiquitinated FANCD2 paralog required for DNA repair. *Cell*, **129**, 289–301.
- Sims,A.E., Spiteri,E., Sims,R.J. 3rd., Arita,A.G., Lach,F.P., Landers,T., Wurm,M., Freund,M., Nevling,K., Hanenberg,H. *et al.* (2007) FANCI is a second monoubiquitinated member of the Fanconi anemia pathway. *Nat. Struct. Mol. Biol.*, **14**, 564–567.
- Dorsman,J.C., Levitus,M., Rockx,D., Roimans,M.A., Oostra,A.B., Haitjema,A., Bakker,S.T., Steltenpool,J., Schuler,D., Mohan,S. *et al.* (2007) Identification of the Fanconi anemia complementation group I gene, FANCI. *Cell Oncol.*, **29**, 211–218.
- Garcia-Higuera,I., Taniguchi,T., Ganesan,S., Meyn,M.S., Timmers,C., Hejna,J., Grompe,M. and D'Andrea,A.D. (2001) Interaction of the Fanconi anemia proteins and BRCA1 in a common pathway. *Mol. Cell*, **7**, 249–262.
- Matsushita,N., Kitao,H., Ishiai,M., Nagashima,N., Hirano,S., Okawa,K., Ohta,T., Yu,D.S., McHugh,P.J., Hickson,I.D. *et al.* (2005) A FANCD2-monoubiquitin fusion reveals hidden functions of Fanconi anemia core complex in DNA repair. *Mol. Cell*, **19**, 841–847.
- Ishiai,M., Kitao,H., Smogorzewska,A., Tomida,J., Kinomura,A., Uchida,E., Saberi,A., Kinoshita,E., Kinoshita-Kikuta,E., Koike,T. *et al.* (2008) FANCI phosphorylation functions as a molecular switch to turn on the Fanconi anemia pathway. *Nat. Struct. Mol. Biol.*, **15**, 1138–1146.
- Meetei,A.R., de Winter,J.P., Medhurst,A.L., Wallisch,M., Waisfisz,Q., van de Vrugt,H.J., Oostra,A.B., Yan,Z., Ling,C., Bishop,C.E. *et al.* (2003) A novel ubiquitin ligase is deficient in Fanconi anemia. *Nat. Genet.*, **35**, 165–170.
- Machida,Y.J., Machida,Y., Chen,Y., Gurtan,A.M., Kupfer,G.M., D'Andrea,A.D. and Dutta,A. (2006) UBE2T is the E2 in the Fanconi anemia pathway and undergoes negative autoregulation. *Mol. Cell*, **23**, 589–596.
- Alpi,A.F., Pace,P.E., Babu,M.M. and Patel,K.J. (2008) Mechanistic insight into site-restricted monoubiquitination of FANCD2 by Ubc2t, FANCL, and FANCI. *Mol. Cell*, **32**, 767–777.
- Bradford,M.M. (1976) A rapid and sensitive method for the quantitation of microgram quantities of protein utilizing the principle of protein-dye binding. *Anal. Biochem.*, **72**, 248–254.
- Iwasaki,H., Takahagi,M., Nakata,A. and Shinagawa,H. (1992) *Escherichia coli* RuvA and RuvB proteins specifically interact with Holliday junctions and promote branch migration. *Genes Dev.*, **6**, 2214–2220.
- Yokoyama,H., Kurumizaka,H., Ikawa,S., Yokoyama,S. and Shibata,T. (2003) Holliday junction binding activity of the human Rad51B protein. *J. Biol. Chem.*, **278**, 2767–2772.
- Horikoshi,N., Morozumi,Y., Takaku,M., Takizawa,Y. and Kurumizaka,H. (2010) Holliday junction-binding activity of human SPF45. *Genes Cells*, **5**, 373–383.
- Yuan,F., Hokayem,E.I. J., Zhou,W. and Zhang,Y. (2009) FANCI protein binds to DNA and interacts with FANCD2 to recognize branched structures. *J. Biol. Chem.*, **284**, 24442–24452.
- Longerich,S., San Filippo,J., Liu,D. and Sung,P. (2009) FANCI binds branched DNA and is monoubiquitinated by UBE2T-FANCL. *J. Biol. Chem.*, **284**, 23182–23186.
- Andreassen,P.R., D'Andrea,A.D. and Taniguchi,T. (2004) ATR couples FANCD2 monoubiquitination to the DNA-damage response. *Genes Dev.*, **18**, 1958–1963.
- Joo,W., Xu,G., Persky,N.S., Smogorzewska,A., Rudge,D.G., Buzovetsky,O., Elledge,S.J. and Pavletich,N.P. (2011) Structure of the FANCI-FANCD2 complex: insights into the Fanconi anemia DNA repair pathway. *Science*, **333**, 312–316.
- Sobeck,A., Stone,S. and Hoatlin,M.E. (2007) DNA structure-induced recruitment and activation of the Fanconi anemia pathway protein FANCD2. *Mol. Cell Biol.*, **27**, 4283–4292.
- Cohn,M.A. and D'Andrea,A.D. (2008) Chromatin recruitment of DNA repair proteins: lessons from the fanconi anemia and double-strand break repair pathways. *Mol. Cell*, **32**, 306–312.
- Huang,M. and D'Andrea,A.D. (2010) A new nuclease member of the FAN club. *Nat. Struct. Mol. Biol.*, **17**, 926–928.
- Kratz,K., Schöpf,B., Kaden,S., Sendoel,A., Eberhard,R., Lademann,C., Cannavó,E., Sartori,A.A., Hengartner,M.O. and Jiricny,J. (2010) Deficiency of FANCD2-associated nuclease KIAA1018/FAN1 sensitizes cells to interstrand crosslinking agents. *Cell*, **142**, 77–88.

27. MacKay,C., Déclais,A.C., Lundin,C., Agostinho,A., Deans,A.J., MacArtney,T.J., Hofmann,K., Gartner,A., West,S.C., Helleday,T. *et al.* (2010) Identification of KIAA1018/FAN1, a DNA repair nuclease recruited to DNA damage by monoubiquitinated FANCD2. *Cell*, **142**, 65–76.
28. Liu,T., Ghosal,G., Yuan,J., Chen,J. and Huang,J. (2010) FAN1 acts with FANCI-FANCD2 to promote DNA interstrand cross-link repair. *Science*, **329**, 693–696.
29. Yoshikiyo,K., Kratz,K., Hirota,K., Nishihara,K., Takata,M., Kurumizaka,H., Horimoto,S., Takeda,S. and Jiricny,J. (2010) KIAA1018/FAN1 nuclease protects cells against genomic instability induced by interstrand cross-linking agents. *Proc. Natl Acad. Sci. USA*, **107**, 21553–21557.
30. Fekairi,S., Scaglione,S., Chahwan,C., Taylor,E.R., Tissier,A., Coulon,S., Dong,M.Q., Ruse,C., Yates,J.R. 3rd, Russell,P. *et al.* (2009) Human SLX4 is a Holliday junction resolvase subunit that binds multiple DNA repair/recombination endonucleases. *Cell*, **138**, 78–89.
31. Svendsen,J.M., Smogorzewska,A., Sowa,M.E., O'Connell,B.C., Gygi,S.P., Elledge,S.J. and Harper,J.W. (2009) Mammalian BTBD12/SLX4 assembles a Holliday junction resolvase and is required for DNA repair. *Cell*, **138**, 63–77.
32. Yamamoto,K.N., Kobayashi,S., Tsuda,M., Kurumizaka,H., Takata,M., Kono,K., Jiricny,J., Takeda,S. and Hirota,K. (2011) Involvement of SLX4 in interstrand cross-link repair is regulated by the Fanconi anemia pathway. *Proc. Natl Acad. Sci. USA*, **108**, 6492–6496.

【第53回日本小児血液・がん学会学術集会】シンポジウム1：本邦における骨髄不全症候群の現状

リバージョン・モザイク型 Fanconi 貧血の診断と臨床

矢部みはる¹，矢部 普正^{2*}

¹東海大学付属病院臨床検査学・細胞移植再生医療科

²東海大学付属病院細胞移植再生医療科

要 旨

Fanconi 貧血 (FA) は種々の身体異常と小児期に発症する骨髄不全，白血化や高発がんを特徴とするまれな遺伝性疾患で，*FANCA* から *FANCP* に到る 15 個という多数の遺伝子異常が報告されている。細胞生物学的にはマイトマイシン (mitomycin C: MMC) などの DNA 架橋剤に対する高い感受性を特徴とする。FA 患者の中にはこうした DNA 架橋剤の感受性が正常化したリンパ球の混在する体細胞モザイク状態が観察され，その分子機構として，遺伝子の変異配列の野生型配列への復帰や，代償性変異により蛋白機能が回復した造血細胞クローンが増大する状態，すなわち「リバージョン・モザイク (reversion mosaicism)」で説明されている。リバージョンを起こしたクローンの増大がリンパ球で著しいと，通常のリンパ球の染色体断裂などの異常がみられず，皮膚などの線維芽細胞を用いた遺伝子検索で初めて確定診断にいたることが多く，FA の診断を極めて困難にしている。

キーワード：Fanconi 貧血，染色体不安定性，リバージョン・モザイク，造血細胞移植

Key words: fanconi anemia, chromose instability, reversion mosaicism, hematopoietic stem cell transplantation

はじめに

スイスの小児科医 Fanconi は 1927 年に家族性の貧血と身体奇形を特徴とする兄弟例を報告し，ファンコニ貧血 (Fanconi anemia: FA) と命名した¹⁾。1964 年，Schroeder らは，FA の患者リンパ球に染色体異常がみられることを発見し²⁾，さらに，佐々木らは，この染色体異常が，MMC などの DNA 架橋剤によって，著しく増加することを見だし，本疾患の原因が染色体不安定性にあることを明らかにした³⁾。FA は遺伝的にも多様な疾患であり，既知の 13 の責任遺伝子の他に，2010 年の FA 国際シンポジウムで認められた *FANCO* に加え，*FANCP* に到る 15 個という多数の遺伝子異常が報告されている。日本小児血液学会の 1988 年～2005 年の全国登録データによれば，1,411 例の再生不良性貧血のうち 89 例が FA で，先天性骨髄不全症の中では Diamond-Blackfan 貧血 (98 例) に次いで多く，全登録例の約 6% を占めていた⁴⁾。しかしながら，一部の FA 患者においては，DNA 架橋剤への感受性が正常化し，全く断裂が認められないリンパ球の混在する体細胞モザイク状態がみられ，FA の診断が極めて困難である。このようなリバージョンを生じたリンパ球はアルキル化剤などの化学療法剤にも抵抗性であるため，前処置を弱めた FA の造血細胞移植に際しては，拒絶やキメラとなる可能性がある。リンパ球にリバージョン・モザイクを認めた症例を中心に，FA

の診断，造血細胞移植を含めた臨床像につき紹介する。

I Fanconi 貧血蛋白群が形成する BRCA 経路

FA は 13 の責任遺伝子に加え⁵⁾ *FANCO*，*FANCP* に到る 15 個という多数の遺伝子異常が報告されている。*FANCD1*，*FANCD2*，*FANCD3*，*FANCD4*，*FANCD5*，*FANCD6*，*FANCD7*，*FANCD8*，*FANCD9*，*FANCD10*，*FANCD11*，*FANCD12*，*FANCD13* はそれぞれ家族性乳がん遺伝子タンパク群の *BRCA2*，*BRIP1*，*PALB2* と同一であり，ヘテロ接合体では FA を発症しないが，発がんリスクの増加がみられる。これらの FA 蛋白群は図 1 に示すように共通のネットワー

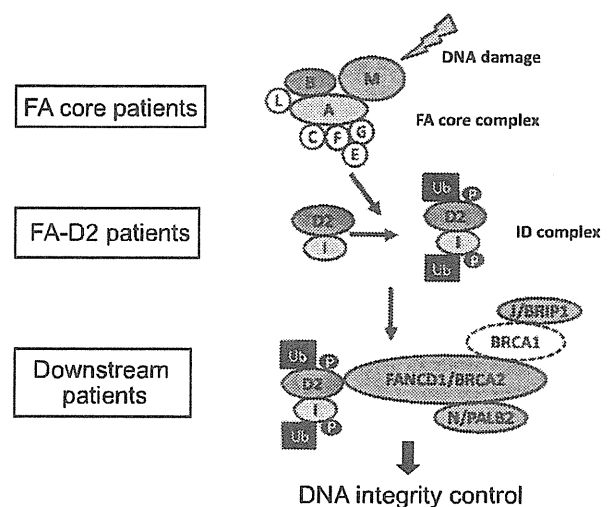


Figure 1 Fanconi anemia-BRCA pathway

The FA proteins represented by A, B, C, D ... N. Ub: ubiquitin
P: phosphoric acid

2012年7月24日受付，2012年7月24日受理

* 別刷請求先：〒259-1193 神奈川県伊勢原市下糟屋143

東海大学付属病院臨床検査学・細胞移植再生医療科 矢部普正

E-mail: miharu@is.icc.u-tokai.ac.jp